

The electromagnetic symmetry sphere: a framework for energy, momentum, spin and other electromagnetic quantities

Sebastian Golat,^{*} Alex J. Vernon, and Francisco J. Rodríguez-Fortuño[†]
*Department of Physics, King's College London, Strand, London WC2R 2LS, UK and
 London Centre for Nanotechnology*
 (Dated: May 27, 2024)

Electromagnetic quantities such as energy density, momentum, spin, and helicity bring meaning and intuition to electromagnetism and possess intricate interrelations, particularly prominent in complex non-paraxial near-fields. These quantities are conventionally expressed using electric and magnetic field vectors, yet the electric-magnetic basis is one among other often overlooked alternatives, including parallel-antiparallel and right-left-handed helicity bases, related to the parity and duality symmetries of electromagnetism. Projecting time-harmonic electromagnetic fields into a variety of bases allows re-interpreting established quantities and reveals underlying mathematical structures: a Bloch sphere which describes asymmetries in electromagnetic energy, a systematic path to unify and uncover relations between electromagnetic quantities, and the unlocking of symmetry-driven equations in light-matter interaction.

Introduction — Modern nanophotonics explores structured near fields in a non-paraxial regime, revealing phenomena like complex 3D polarizations, spin-orbit interactions, and oscillating energy flows, often leading to novel applications. Many physical quantities are defined and invoked in our attempts to gain intuition and give meaning to the field's behavior, such as the field's energy density, energy flow, linear momenta, angular momenta, helicity, and many others, which—remarkably often—are quadratic quantities in the fields. In-depth study of these quantities often reveals intricate relations between them [1–8]. In this Letter we propose an organising framework whose starting point is the underlying symmetries of electromagnetism, allowing quadratic quantities to be visualised on a Poincaré/Bloch sphere, and revealing intricate relations between them.

Bispinor formalism — Bispinors, combining electric and magnetic fields into a single ‘wavefunction’ ψ , offer profound insights into electromagnetism's mathematical structure [9–11]. The foundation of this work is to fully embrace that, for monochromatic light, these bispinors live in a $\mathbb{C}^3 \times \mathbb{C}^2 \times \mathbb{L}^2(\mathbb{R}^3)$ vector space: \mathbb{C}^3 due to \mathbf{E} and \mathbf{H} being 3-dimensional complex phasors, \mathbb{C}^2 because \mathbf{E} and \mathbf{H} have a relative amplitude and phase with respect to each other, and $\mathbb{L}^2(\mathbb{R}^3)$ because each component is

a square-integrable function of position (or momentum). In the literature, these bispinors are typically written in a basis in \mathbb{C}^2 space $\psi = \frac{1}{2}(\sqrt{\varepsilon}\mathbf{E}, \sqrt{\mu}\mathbf{H})^\top$ which separates electric and magnetic fields. But like any other \mathbb{C}^2 space, isomorphic with the Jones vector that describes 2D plane wave polarisation, different choices of basis can be made (see fig. 1). Viewing an electromagnetic wave as composed of electric and magnetic fields is just as valid as considering it constituted by parallel and anti-parallel, or right and left-handed fields (see supplementary for a step-by-step justification):

$$\begin{aligned}\psi_{\text{EM}}(\mathbf{r}) &= \begin{pmatrix} \mathbf{F}_e \\ \mathbf{F}_m \end{pmatrix} = \frac{1}{2} \begin{pmatrix} \sqrt{\varepsilon}\mathbf{E} \\ \sqrt{\mu}\mathbf{H} \end{pmatrix}, \\ \psi_{\text{PA}}(\mathbf{r}) &= \begin{pmatrix} \mathbf{F}_p \\ \mathbf{F}_a \end{pmatrix} = \frac{1}{2\sqrt{2}} \begin{pmatrix} \sqrt{\varepsilon}\mathbf{E} + \sqrt{\mu}\mathbf{H} \\ \sqrt{\varepsilon}\mathbf{E} - \sqrt{\mu}\mathbf{H} \end{pmatrix}, \\ \psi_{\text{RL}}(\mathbf{r}) &= \begin{pmatrix} \mathbf{F}_R \\ \mathbf{F}_L \end{pmatrix} = \frac{1}{2\sqrt{2}} \begin{pmatrix} \sqrt{\varepsilon}\mathbf{E} + i\sqrt{\mu}\mathbf{H} \\ \sqrt{\varepsilon}\mathbf{E} - i\sqrt{\mu}\mathbf{H} \end{pmatrix}.\end{aligned}\quad (1)$$

These three bases: electric-magnetic (EM), parallel-antiparallel (PA) and right-left handed (RL), relate to the fundamental electromagnetic symmetries: parity inversion $\hat{P}: \mathbf{r} \mapsto -\mathbf{r}$, time reversal $\hat{T}: t \mapsto -t$, and discrete duality transformation \hat{D} . These act on the fields as

$$\begin{aligned}\hat{D}: (\sqrt{\varepsilon}\mathbf{E}, \sqrt{\mu}\mathbf{H})^\top &\mapsto (\sqrt{\mu}\mathbf{H}, -\sqrt{\varepsilon}\mathbf{E})^\top, \\ \hat{P}: (\sqrt{\varepsilon}\mathbf{E}, \sqrt{\mu}\mathbf{H})^\top &\mapsto (-\sqrt{\varepsilon}\mathbf{E}, \sqrt{\mu}\mathbf{H})^\top, \\ \hat{T}: (\sqrt{\varepsilon}\mathbf{E}, \sqrt{\mu}\mathbf{H})^\top &\mapsto (\sqrt{\varepsilon}\mathbf{E}^*, -\sqrt{\mu}\mathbf{H}^*)^\top,\end{aligned}\quad (2)$$

so \hat{D} is a 90 degree rotation in \mathbb{C}^2 space, while \hat{P} is a mirror symmetry inverting the \mathbf{E} axis. The components of the EM basis are eigenvectors of the \hat{P} operator, RL basis of the \hat{D} operator, and PA basis of the combined $\hat{P}\hat{D}$ operator. Note that the fields \mathbf{F}_R and \mathbf{F}_L are similar to Riemann-Silberstein vectors [12–14] but here defined using complex phasors \mathbf{E} and \mathbf{H} .

Field projections — Any electromagnetic field (\mathbf{E}, \mathbf{H}) can be decomposed into a sum of two components, based

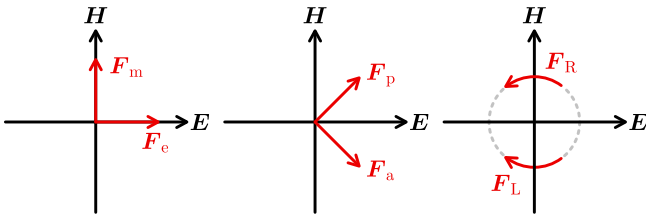


FIG. 1. Components of the bispinor when represented in electric-magnetic (EM), parallel-antiparallel (PA) and right-left handed (RL) bases, drawn with respect to \mathbf{E} and \mathbf{H} vector-valued axes of the traditional EM basis.

on the different bases in \mathbb{C}^2 space:

$$\begin{aligned} \mathbf{E} &= \mathbf{E}_e + \mathbf{E}_m = \mathbf{E} + \mathbf{0} \\ &= \mathbf{E}_p + \mathbf{E}_a = \frac{\mathbf{E} + \eta \mathbf{H}}{2} + \frac{\mathbf{E} - \eta \mathbf{H}}{2} \\ &= \mathbf{E}_R + \mathbf{E}_L = \frac{\mathbf{E} + i\eta \mathbf{H}}{2} + \frac{\mathbf{E} - i\eta \mathbf{H}}{2}, \end{aligned} \quad (3)$$

with the corresponding $\mathbf{H}_e = \mathbf{0}, \mathbf{H}_m = \mathbf{H}, \mathbf{H}_{p,a} = \pm \mathbf{E}_{p,a}/\eta$ and $\mathbf{H}_{R,L} = \mp i \mathbf{E}_{R,L}/\eta$, and $\eta = \sqrt{\mu/\varepsilon}$. These pairs $(\mathbf{E}_i, \mathbf{H}_i)$ represent the projection of the total electromagnetic field into each basis vector in \mathbb{C}^2 space, with $i = (e, m, p, a, R, L)$. For example, a linearly polarised field with $\mathbf{E} = E_0 \hat{x}$ and $\mathbf{H} = E_0 \hat{y}/\eta$ may be decomposed in the PA basis as the sum of parallel fields $(\mathbf{E}_p, \mathbf{H}_p) = E_0(\frac{\hat{x}+\hat{y}}{2}, \frac{\hat{x}+\hat{y}}{2\eta})$, which have $\mathbf{F}_a = 0$, plus antiparallel ones $(\mathbf{E}_a, \mathbf{H}_a) = E_0(\frac{\hat{x}-\hat{y}}{2}, -\frac{\hat{x}-\hat{y}}{2\eta})$, which have $\mathbf{F}_p = 0$. Each of these pairs of simultaneous electric and magnetic fields, given by $(\mathbf{E}_i, \mathbf{H}_i)$, are mathematical projections, not physically realizable in vacuum, except for the pairs $(\mathbf{E}_R, \mathbf{H}_R)$ and $(\mathbf{E}_L, \mathbf{H}_L)$ which correspond to realizable pure helicity fields [3, 15]. The total electromagnetic energy density W is given by the norm $\|\psi\|^2$. Thanks to orthogonality and Parseval's identity, the energy density W is the sum of the squared norm of each of the two ψ components in any of the three bases. Therefore, W , a quadratic quantity that is generally not linear with the fields, can be obtained *by linear addition* in three different ways $W = W_e + W_m = W_p + W_a = W_R + W_L$, of which the first is well-known. A similar argument applies for the total spin angular momentum $\mathbf{S} = \mathbf{S}_e + \mathbf{S}_m = \mathbf{S}_p + \mathbf{S}_a = \mathbf{S}_L + \mathbf{S}_R$, and total stress tensor $\mathbf{T} = \mathbf{T}_e + \mathbf{T}_m = \mathbf{T}_p + \mathbf{T}_a = \mathbf{T}_L + \mathbf{T}_R$, by changing the dot product implicit in $W_i = |\mathbf{F}_i|^2 = \mathbf{F}_i^* \cdot \mathbf{F}_i$ into a cross or outer product. The individual components W_i, \mathbf{S}_i and \mathbf{T}_i (with a subscript $i = (e, m, p, a, R, L)$ corresponding to each of the six field projections) are defined laconically using the corresponding field coefficients \mathbf{F}_i from eq. (1), and can also be understood as the energy, spin, and stress tensor of each projection (using \mathbf{E}_i and \mathbf{H}_i from eq. (3)):

$$\begin{aligned} W_i &= \mathbf{F}_i^* \cdot \mathbf{F}_i = \frac{1}{4}(\varepsilon \mathbf{E}_i^* \cdot \mathbf{E}_i + \mu \mathbf{H}_i^* \cdot \mathbf{H}_i), \\ i\omega \mathbf{S}_i &= \mathbf{F}_i^* \times \mathbf{F}_i = \frac{1}{4}(\varepsilon \mathbf{E}_i^* \times \mathbf{E}_i + \mu \mathbf{H}_i^* \times \mathbf{H}_i), \\ \mathbf{T}_i + W_i \mathbf{I} &= \mathbf{F}_i^* \odot \mathbf{F}_i = \frac{1}{4}(\varepsilon \mathbf{E}_i^* \odot \mathbf{E}_i + \mu \mathbf{H}_i^* \odot \mathbf{H}_i), \end{aligned} \quad (4)$$

where \odot represents the symmetric outer product defined as $\mathbf{A} \odot \mathbf{B} = \mathbf{A} \otimes \mathbf{B} + \mathbf{B} \otimes \mathbf{A}$, and \otimes is outer product.

Table of quadratic quantities — Even more interesting is the *subtraction* of corresponding quantities W_i, \mathbf{S}_i and \mathbf{T}_i , yielding a collection of physically meaningful quadratic quantities that are even or odd with respect to each of the symmetries. These are listed exhaustively in table I. A more rigorous mathematical motivation for performing these subtractions is given in the supplementary. Remarkably, one can find familiar quadratic quanti-

	Quantity	Definition	\hat{D}	\hat{P}	\hat{T}
W_0	W	$\frac{1}{4}(\varepsilon \mathbf{E} ^2 + \mu \mathbf{H} ^2)$	+	+	+
W_1	$W_e - W_m$	$\frac{1}{4}(\varepsilon \mathbf{E} ^2 - \mu \mathbf{H} ^2)$	-	+	+
W_2	$W_a - W_p$	$-\omega \mathfrak{S}_{\text{reac}} = -\frac{1}{2} \Re(\sqrt{\varepsilon \mu} \mathbf{E}^* \cdot \mathbf{H})$	-	-	-
W_3	$W_R - W_L$	$\omega \mathfrak{S} = -\frac{1}{2} \Im(\sqrt{\varepsilon \mu} \mathbf{E}^* \cdot \mathbf{H})$	+	-	+
\mathbf{p}_0	\mathbf{p}	$\frac{1}{4\omega} \Im[\varepsilon \mathbf{E}^* \cdot (\nabla) \mathbf{E} + \mu \mathbf{H}^* \cdot (\nabla) \mathbf{H}]$	+	-	-
\mathbf{p}_1	$\mathbf{p}_e - \mathbf{p}_m$	$\frac{1}{4\omega} \Im[\varepsilon \mathbf{E}^* \cdot (\nabla) \mathbf{E} - \mu \mathbf{H}^* \cdot (\nabla) \mathbf{H}]$	-	-	-
\mathbf{p}_2	$\mathbf{p}_a - \mathbf{p}_p$	$\frac{1}{4\omega} \Im\{\sqrt{\varepsilon \mu} [\mathbf{E} \cdot (\nabla) \mathbf{H}^* - \mathbf{H}^* \cdot (\nabla) \mathbf{E}]\}$	-	+	+
\mathbf{p}_3	$\mathbf{p}_R - \mathbf{p}_L$	$\frac{1}{4\omega} \Re\{\sqrt{\varepsilon \mu} [\mathbf{E} \cdot (\nabla) \mathbf{H}^* - \mathbf{H}^* \cdot (\nabla) \mathbf{E}]\}$	+	+	-
\mathbf{S}_0	\mathbf{S}	$\frac{1}{4\omega} \Im(\varepsilon \mathbf{E}^* \times \mathbf{E} + \mu \mathbf{H}^* \times \mathbf{H})$	+	+	-
\mathbf{S}_1	$\mathbf{S}_e - \mathbf{S}_m$	$\frac{1}{4\omega} \Im(\varepsilon \mathbf{E}^* \times \mathbf{E} - \mu \mathbf{H}^* \times \mathbf{H})$	-	+	-
\mathbf{S}_2	$\mathbf{S}_a - \mathbf{S}_p$	$\frac{1}{\omega c} \Im \mathbf{\Pi} = \frac{1}{2\omega} \Im(\sqrt{\varepsilon \mu} \mathbf{E} \times \mathbf{H}^*)$	-	-	+
\mathbf{S}_3	$\mathbf{S}_R - \mathbf{S}_L$	$\frac{1}{\omega c} \Re \mathbf{\Pi} = \frac{1}{2\omega} \Re(\sqrt{\varepsilon \mu} \mathbf{E} \times \mathbf{H}^*)$	+	-	-
\mathbf{T}_0	\mathbf{T}	$\frac{1}{4}(\varepsilon \mathbf{E}^* \odot \mathbf{E} + \mu \mathbf{H}^* \odot \mathbf{H}) - W_0 \mathbf{I}$	+	+	+
\mathbf{T}_1	$\mathbf{T}_e - \mathbf{T}_m$	$\frac{1}{4}(\varepsilon \mathbf{E}^* \odot \mathbf{E} - \mu \mathbf{H}^* \odot \mathbf{H}) - W_1 \mathbf{I}$	-	+	+
\mathbf{T}_2	$\mathbf{T}_a - \mathbf{T}_p$	$-\frac{1}{2} \Re(\sqrt{\varepsilon \mu} \mathbf{E}^* \odot \mathbf{H}) - W_2 \mathbf{I}$	-	-	-
\mathbf{T}_3	$\mathbf{T}_R - \mathbf{T}_L$	$-\frac{1}{2} \Im(\sqrt{\varepsilon \mu} \mathbf{E}^* \odot \mathbf{H}) - W_3 \mathbf{I}$	+	-	+

TABLE I. Quadratic quantities in the fields. We indicate symmetries under D, P, and T transformations. The symmetric outer product is to be understood as $\mathbf{A} \odot \mathbf{B} \equiv \mathbf{A} \otimes \mathbf{B} + \mathbf{B} \otimes \mathbf{A}$ where \otimes is the outer product, while $\mathbf{A} \cdot (\nabla) \mathbf{B} \equiv \sum_i (A_i \nabla B_i)$.

ties “hidden” within table I, such as the complex Poynting vector $\mathbf{\Pi} = \frac{1}{2} \mathbf{E} \times \mathbf{H}^*$ (whose real and imaginary parts appear in $\mathbf{S}_R - \mathbf{S}_L$ and $\mathbf{S}_a - \mathbf{S}_p$ respectively), the electromagnetic helicity \mathfrak{S} , known to be proportional to $W_R - W_L$ [16–18] and chiral momentum $\mathbf{p}_R - \mathbf{p}_L$ [7, 10]. Likewise reactive helicity $\mathfrak{S}_{\text{reac}}$, a quantity recently explored in Ref. [19] and proportional to magnetoelectric energy density [10], appears in $W_a - W_p$. We believe this provides a systematic and elegant symmetry-based way to interpret these quantities. In some cases, similar decompositions were made in different contexts, such as the helicity decomposition of the Poynting vector [3] related to \mathbf{S}_3 , and that of the local wavevector [18] related to \mathbf{p}_0 . Table I expresses all quantities in the familiar EM basis (i.e. in terms of electric and magnetic fields). But we can break free of such EM bias and express the same quantities in other bases, by using \mathbf{F}_i from eq. (1). This leads to simpler expressions as demonstrated for the energy densities in table II (the extension to the other quadratic quantities is given in the supplementary). A clear pattern emerges in Table II, which reveals the isomorphism of the \mathbb{C}^2 space of ψ , with the Jones vector space of 2D polarisations: the quadratic quantities, expressed in different bases, exhibit an *exact* mathematical analogy with the Stokes polarisation parameters, a fact that motivates our subscript labelling $A = 0, 1, 2, 3$ in the first column of tables I and II.

Bloch sphere — Given the mathematical analogy with Stokes parameters, it is natural to plot the real vector $\mathbf{W} = (W_1, W_2, W_3)$ in W -space. As with Stokes

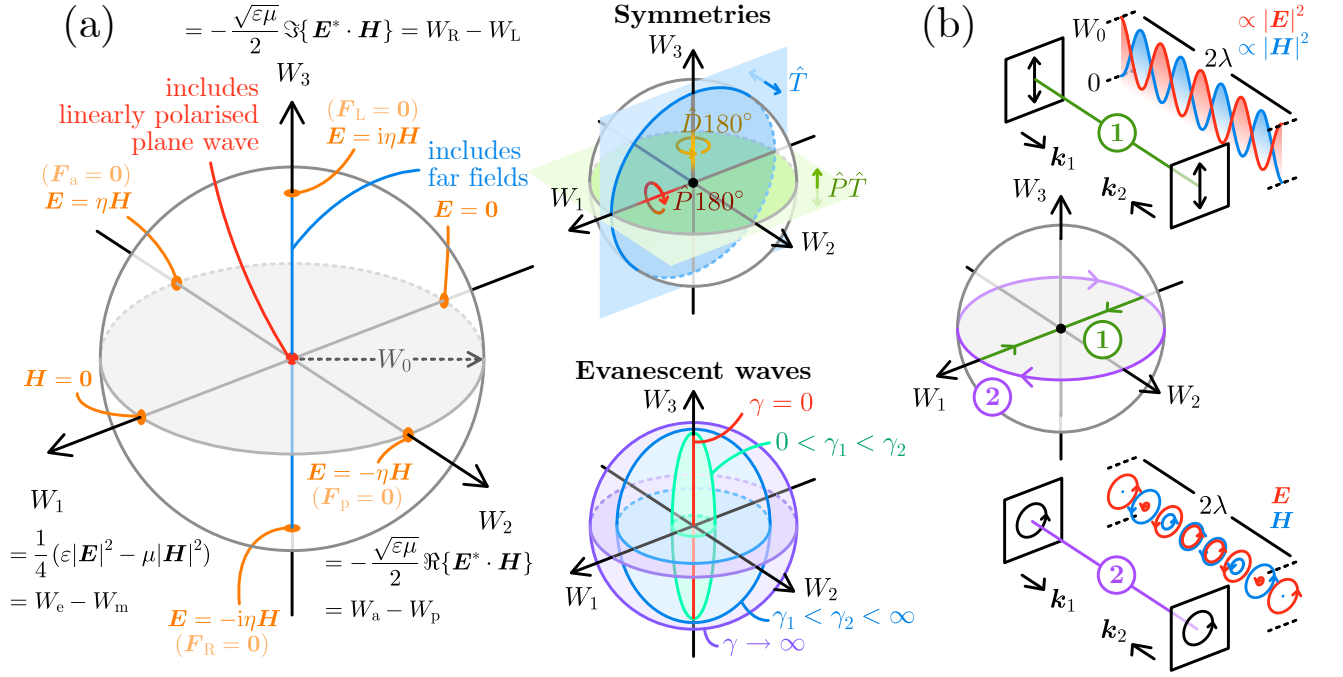


FIG. 2. (a) The energy symmetry sphere (ESS), axes defined by the energy densities W_{1-3} , and its special points (orange). Far fields lie along the W_3 axis while a linearly polarised plane wave (preserving all symmetries) resides at the sphere centre. The upper inset depicts the effect of symmetry transformations on a field plotted in the sphere (\hat{D} and \hat{P} transformations cause 180° rotations about the W_3 and W_1 axes respectively, \hat{T} and $\hat{P}\hat{T}$ operations respectively reflect fields through the W_1, W_3 and W_1, W_2 planes). The lower inset shows how evanescent waves can map to any point on an ellipsoid surface within the ESS, depending on the decay constant. (b) Traces on the ESS produced by two standing wave examples (top and bottom). The upper example (green line) maps the optical axis (a 2λ section) of two counter-propagating plane waves with identical linear polarisations to the sphere, giving a trace along the W_1 axis as energy is shared space-periodically among \mathbf{E} and \mathbf{H} . In the lower example, a standing wave where both plane waves are circularly polarised with the same spin direction (corresponding to the purple line) produces a trace around the equator of the ESS. Arrowheads (on the polarisation circles) indicate the phase of the \mathbf{E} and \mathbf{H} fields at various points along the standing wave, showing that the time-dependent electric and magnetic field vectors are always (anti)parallel (hence the ESS trace lies at $W_3 = 0$).

	EM basis	PA basis	RL basis
W_0	$\mathbf{F}_e^* \cdot \mathbf{F}_e + \mathbf{F}_m^* \cdot \mathbf{F}_m$	$\mathbf{F}_a^* \cdot \mathbf{F}_a + \mathbf{F}_p^* \cdot \mathbf{F}_p$	$\mathbf{F}_R^* \cdot \mathbf{F}_R + \mathbf{F}_L^* \cdot \mathbf{F}_L$
W_1	$\mathbf{F}_e^* \cdot \mathbf{F}_e - \mathbf{F}_m^* \cdot \mathbf{F}_m$	$2\Re(\mathbf{F}_p^* \cdot \mathbf{F}_a)$	$2\Re(\mathbf{F}_R^* \cdot \mathbf{F}_L)$
W_2	$-2\Re(\mathbf{F}_e^* \cdot \mathbf{F}_m)$	$\mathbf{F}_a^* \cdot \mathbf{F}_a - \mathbf{F}_p^* \cdot \mathbf{F}_p$	$2\Im(\mathbf{F}_R^* \cdot \mathbf{F}_L)$
W_3	$-2\Im(\mathbf{F}_e^* \cdot \mathbf{F}_m)$	$2\Im(\mathbf{F}_p^* \cdot \mathbf{F}_a)$	$\mathbf{F}_R^* \cdot \mathbf{F}_R - \mathbf{F}_L^* \cdot \mathbf{F}_L$

TABLE II. Energy densities in different bases, revealing the similarity with Stokes vectors (for an extension to the other quadratic quantities see supplementary).

parameters, this vector is contained on a sphere of radius W_0 , analogous to the Poincare or Bloch sphere. We term this the *energy symmetry sphere*, depicted in fig. 2, as it reveals how the energy is distributed among the symmetries. Time-reversal \hat{T} mirrors the sphere on the (W_1, W_3) plane, parity \hat{P} rotates it 180 degrees around the W_1 axis, and duality \hat{D} rotates it around W_3 . Unlike the Stokes parameters in the Poincare sphere, which only describe 2D polarisation, the symmetry sphere can describe *any* electromagnetic field (\mathbf{E}, \mathbf{H}) , including non-

paraxial, structured and near-fields, with arbitrary three-dimensional polarisation. The absolute spatial orientation of polarisation ellipses is not relevant to the energy symmetry sphere, but the relative orientation and phase between \mathbf{E} and \mathbf{H} plays a crucial role. Unlike the Poincare sphere, fully polarised electromagnetic fields can exist anywhere in the surface *or inside* the sphere. The distance to the origin indicates how asymmetrically-distributed the energy is. Linearly polarised plane waves lie at the origin of the symmetry sphere, with maximum symmetry ($W_e = W_m = W_p = W_a = W_R = W_L = W/2$). All possible homogeneous plane waves and paraxial far fields exist along the W_3 axis ($W_1 = W_2 = 0$) with circular polarisation at the poles, while homogeneous evanescent waves can stray away from the W_3 axis, more so when more confined. The states at the very surface of the symmetry sphere (where $W_1^2 + W_2^2 + W_3^2 = W_0^2$) correspond to maximum-asymmetry between the energies in the two orthogonal states of some basis in \mathbb{C}^2 space. As shown in the supplementary, this corresponds to $\mathbf{E} = \delta\eta\mathbf{H}$ with δ a complex scalar. This means that

states in the surface have fewer degrees of freedom, the electric and magnetic fields are proportional and share the same polarisation structure. This was pointed out for pure helicity fields [13, 14], which is a particular case of being at the surface (north and south poles). In contrast, any states *inside* the sphere must have linearly independent fields. Figure 2 depicts special points on the surface where $\mathbf{F}_i = 0$ and hence $W_i = 0$ for $i = (e, m, p, a, R, L)$, corresponding to the field projections from eq. (3). The polar angle with respect to the axis joining the origin to any $\mathbf{F}_i = 0$ point on the surface is related to the amplitude ratio between the two orthogonal components in that basis, while the azimuthal angle around the axis represents their phase difference (see supplementary).

Any spatial profile of electromagnetic fields $(\mathbf{E}(\mathbf{r}), \mathbf{H}(\mathbf{r}))$ can be mapped into the symmetry sphere, with every position \mathbf{r} mapped to a point $\mathbf{W}(\mathbf{r})$ within the sphere. Doing this on simple standing waves leads to simple curves as in fig. 2(b), while doing it on more complicated fields, such as dipolar fields, leads to intriguing and sometimes beautiful patterns (see supplementary).

An electromagnetic field (\mathbf{E}, \mathbf{H}) cannot be superimposed onto its mirror image (accounting for the pseudovector nature of \mathbf{H}) if either $W_3 \neq 0$ or $W_2 \neq 0$, so both quantities (helicity and reactive helicity) represent a form of time-averaged chirality. Indeed, chiral gradient forces are directed along ∇W_3 and ∇W_2 for chiral and non-reciprocal particles, respectively [20]. While both $W_{2,3}$ change sign under parity, only W_2 changes sign under time reversal, making W_2 PT-symmetric [10]. The energy symmetry sphere requirement $W_1^2 + W_2^2 + W_3^2 \leq W_0^2$ represents a fundamental limit. For instance, maximum helicity $W_3 = \pm W_0$ is attained when $W_1 = W_2 = 0$, requiring equal electric and magnetic energies, while purely electric or magnetic fields $W_1 = \pm W_0$ (where $\mathbf{H} = 0$ or $\mathbf{E} = 0$) require $W_2 = W_3 = 0$, and hence cannot be locally chiral.

Plane waves and evanescent waves — A deep relationship between the quadratic quantities W_A and the Stokes polarisation parameters \mathcal{S}_A is revealed if we consider a plane wave, whose fields are:

$$\begin{aligned}\sqrt{\varepsilon}\mathbf{E}(\mathbf{r}) &= (0, A_s, -A_p)^\top e^{ikx}, \\ \sqrt{\mu}\mathbf{H}(\mathbf{r}) &= (0, A_p, A_s)^\top e^{ikx}.\end{aligned}\quad (5)$$

The Stokes parameters which describe the polarisation of this plane wave are defined as

$$\begin{aligned}\mathcal{S}_0 &= |A_p|^2 + |A_s|^2, & \mathcal{S}_2 &= 2\Re(A_p^* A_s), \\ \mathcal{S}_1 &= |A_p|^2 - |A_s|^2, & \mathcal{S}_3 &= 2\Im(A_p^* A_s).\end{aligned}$$

The quadratic quantities from table I evaluated for this simple plane wave field are given in table III, illuminating the relation to the Stokes parameters. As mentioned earlier, plane waves have $W_2 = W_3 = 0$, but also

$\mathcal{S}_1 = \mathcal{S}_2 = 0$. Even more intricate relations appear for an evanescent wave with effective index $n = k_x/k$ (associated to $\kappa = \sqrt{n^2 - 1}$) such that $\mathbf{k} = k(n\hat{\mathbf{x}} + i\kappa\hat{\mathbf{z}})$, with arbitrary polarisation (but still ensuring that $\nabla \cdot \mathbf{E} = \nabla \cdot \mathbf{H} = 0$):

$$\begin{aligned}\sqrt{\varepsilon}\mathbf{E} &= (i\kappa A_p, A_s, -nA_p)^\top e^{i\mathbf{k}\cdot\mathbf{r}}, \\ \sqrt{\mu}\mathbf{H} &= (-i\kappa A_s, A_p, nA_s)^\top e^{i\mathbf{k}\cdot\mathbf{r}},\end{aligned}\quad (6)$$

where $e^{i\mathbf{k}\cdot\mathbf{r}} = e^{iknx - k\kappa z}$ and eq. (5) is recovered when ($n = 1, \kappa = 0$). The quadratic quantities for this evanescent wave are given in table III. Many recent findings related to evanescent waves and guided modes are present in table III, namely, the transverse spin ($\mathcal{S}_0 \cdot \hat{\mathbf{y}}$), associated with spin-momentum locking or spin-orbit interaction of guided modes [11, 21–26], the transverse Poynting vector ($\mathcal{S}_3 \cdot \hat{\mathbf{y}}$), also known as Belinfante’s momentum [10, 27–29], the imaginary Poynting vector structure of evanescent waves in the direction of decay ($\mathcal{S}_2 \cdot \hat{\mathbf{z}}$) [19, 30, 31], and in addition to these, new aspects of evanescent waves are revealed in table III, such as the transverse components of vector $\mathcal{S}_1 = \mathcal{S}_e - \mathcal{S}_m$.

Relating quadratic quantities — The quadratic quantities defined in table I are intimately related to one another via their curl and divergence. Below is a list of curls and divergences of \mathcal{S}_A , \mathbf{p}_A , and \mathcal{T}_A valid in free space. Starting with the spin-like quantities, we have:

$$\begin{aligned}\nabla \times \mathcal{S}_0 &= 2(k\mathcal{S}_3 - \mathbf{p}_0), & \nabla \cdot \mathcal{S}_0 &= 0, \\ \nabla \times \mathcal{S}_1 &= -2\mathbf{p}_1, & \nabla \cdot \mathcal{S}_1 &= +\frac{2}{c}W_2, \\ \nabla \times \mathcal{S}_2 &= -2\mathbf{p}_2, & \nabla \cdot \mathcal{S}_2 &= -\frac{2}{c}W_1, \\ \nabla \times \mathcal{S}_3 &= 2(k\mathcal{S}_0 - \mathbf{p}_3), & \nabla \cdot \mathcal{S}_3 &= 0.\end{aligned}\quad (7)$$

These equations, with divergences seen as continuity conditions, elegantly incorporate many known relations and facts, such as: the Poynting theorem for time-harmonic fields in free space ($\nabla \cdot \mathcal{S}_3 = 0$) and the known fact that reactive power (imaginary Poynting vector $\propto \mathcal{S}_2$ [32, 33]) is the flow of reactive energy $W_1 = W_e - W_m$. The curl equations include the known Belinfante-Rosenfeld decomposition of the real Poynting vector ($\omega c\mathcal{S}_3$) into canonical momentum (\mathbf{p}_0) and spin momentum ($\nabla \times \mathcal{S}_0$) [2, 11, 34–36], and the lesser-known decomposition of total spin (\mathcal{S}_0) into canonical spin ($\propto \mathbf{p}_3$) and Poynting spin ($\nabla \times \mathcal{S}_3$) [7, 10].

Combining the previous results together with the identity $\nabla \times (\nabla \times \mathbf{A}) = \nabla(\nabla \cdot \mathbf{A}) - \nabla^2 \mathbf{A}$ we can obtain the curls of \mathbf{p}_A , while all $\nabla \cdot \mathbf{p}_A = 0$ from eq. (7). Finally, the tensor divergences are:

$$\nabla \cdot \mathcal{T}_{0/3} = 0, \quad \nabla \cdot \mathcal{T}_{1/2} = \mp 2k\omega \mathcal{S}_{2/1}. \quad (8)$$

Equation (7) implies a Helmholtz/Poisson equation for the spin-like quantities with double and zero frequency as follows:

$$\begin{aligned}(\nabla^2 + 4k^2)\mathcal{S}_{0/3} &= 4k\mathbf{p}_{3/0} + 2\nabla \times \mathbf{p}_{0/3}, \\ (\nabla^2 + 0k^2)\mathcal{S}_{1/2} &= \pm \frac{2}{c}\nabla W_{2/1} \pm 2\nabla \times \mathbf{p}_{1/2}.\end{aligned}\quad (9)$$

Quadratic quantity	Plane wave	Evanescent wave
W_0, W_1, W_2, W_3	$\frac{1}{2}\mathcal{S}_0, 0, 0, \frac{1}{2}\mathcal{S}_3$	$\frac{1}{2}e^{-2\kappa z}n^2\mathcal{S}_0, \frac{1}{2}e^{-2\kappa z}\kappa^2\mathcal{S}_1, \frac{1}{2}e^{-2\kappa z}\kappa^2\mathcal{S}_2, \frac{1}{2}e^{-2\kappa z}n^2\mathcal{S}_3$
$\mathcal{S}_0, \mathcal{S}_1, \mathcal{S}_2, \mathcal{S}_3$	$\frac{1}{2\omega} \begin{pmatrix} \mathcal{S}_3 \\ 0 \\ 0 \end{pmatrix}, \begin{pmatrix} 0 \\ 0 \\ 0 \end{pmatrix}, \begin{pmatrix} 0 \\ 0 \\ 0 \end{pmatrix}, \frac{1}{2\omega} \begin{pmatrix} \mathcal{S}_0 \\ 0 \\ 0 \end{pmatrix}$	$\frac{e^{-2\kappa z}}{2\omega} \begin{pmatrix} n\mathcal{S}_3 \\ n\kappa\mathcal{S}_0 \\ 0 \end{pmatrix}, \frac{e^{-2\kappa z}}{2\omega} \begin{pmatrix} 0 \\ n\kappa\mathcal{S}_1 \\ \kappa\mathcal{S}_2 \end{pmatrix}, \frac{e^{-2\kappa z}}{2\omega} \begin{pmatrix} 0 \\ -n\kappa\mathcal{S}_2 \\ \kappa\mathcal{S}_1 \end{pmatrix}, \frac{e^{-2\kappa z}}{2\omega} \begin{pmatrix} n\mathcal{S}_0 \\ -n\kappa\mathcal{S}_3 \\ 0 \end{pmatrix}$
$\mathcal{T}_0, \mathcal{T}_1$	$\frac{1}{2} \begin{pmatrix} -\mathcal{S}_0 & 0 & 0 \\ 0 & 0 & 0 \\ 0 & 0 & 0 \end{pmatrix}, \frac{1}{2} \begin{pmatrix} 0 & 0 & 0 \\ 0 & -\mathcal{S}_1 & -\mathcal{S}_2 \\ 0 & -\mathcal{S}_2 & \mathcal{S}_1 \end{pmatrix}$	$\frac{e^{-2\kappa z}}{2} \begin{pmatrix} -\mathcal{S}_0 & -\kappa\mathcal{S}_3 & 0 \\ -\kappa\mathcal{S}_3 & -\kappa^2\mathcal{S}_0 & 0 \\ 0 & 0 & 0 \end{pmatrix}, \frac{e^{-2\kappa z}}{2} \begin{pmatrix} 0 & 0 & 0 \\ 0 & -n^2\mathcal{S}_1 & -n\mathcal{S}_2 \\ 0 & -n\mathcal{S}_2 & \mathcal{S}_1 \end{pmatrix}$
$\mathcal{T}_2, \mathcal{T}_3$	$\frac{1}{2} \begin{pmatrix} 0 & 0 & 0 \\ 0 & -\mathcal{S}_2 & \mathcal{S}_1 \\ 0 & \mathcal{S}_1 & \mathcal{S}_2 \end{pmatrix}, \frac{1}{2} \begin{pmatrix} -\mathcal{S}_3 & 0 & 0 \\ 0 & 0 & 0 \\ 0 & 0 & 0 \end{pmatrix}$	$\frac{e^{-2\kappa z}}{2} \begin{pmatrix} 0 & 0 & 0 \\ 0 & -n^2\mathcal{S}_2 & n\mathcal{S}_1 \\ 0 & n\mathcal{S}_1 & \mathcal{S}_2 \end{pmatrix}, \frac{e^{-2\kappa z}}{2} \begin{pmatrix} -(1+2\kappa^2)\mathcal{S}_3 & \kappa\mathcal{S}_0 & 0 \\ \kappa\mathcal{S}_0 & -\kappa^2\mathcal{S}_3 & 0 \\ 0 & 0 & 0 \end{pmatrix}$

TABLE III. Representation of quadratic quantities in a plane wave and an evanescent wave. The momenta-like quantities \mathbf{p}_A can be obtained from $\mathbf{p}_A = W_a \Re(\mathbf{k})/\omega$.

This explains why \mathcal{S}_1 and \mathcal{S}_2 , like W_1 and W_2 , are static-like (they tend to zero in the far-field) while \mathcal{S}_0 and \mathcal{S}_3 (total spin and real Poynting vector) form propagating waves that extend into the far-fields, like W_0 and W_3 . A partial version of the first line in eq. (9) was presented in [37], with a claim of equivalence to Maxwell's equations and with calculations of extraordinary spin and momentum which were scrutinised in [38]. In fact, some signs that are crucial to Maxwell's equations do not match those in eq. (7). However, we can define new complex quantities $\mathcal{S}_A \pm i\mathcal{S}_B$, $W_A \pm iW_B$, and $\mathbf{p}_A \pm i\mathbf{p}_B$ which exactly match all signs in Maxwell's equations (see supplementary). Equations (7) to (9) laconically unify many known relations, while others are novel to our knowledge, and we highlight how elegantly and systematically they all arise from the quadratic quantities in table I.

Relativistic interpretation — In relativistic electrodynamics, the full energy-momentum-stress tensor $T^{\mu\nu}$ represents the flux of 4-momentum:

$$(\text{4-momentum flux}) = \begin{pmatrix} \text{energy density} & \text{energy flux}/c \\ c(\text{momentum density}) & \text{momentum flux} \end{pmatrix}.$$

When energy and momentum are conserved, the continuity equation for this tensor becomes $\partial_\nu T^{\mu\nu} = 0$, which can be written in general (no time average) as

$$\begin{pmatrix} \partial_\nu T^{0\nu} \\ \partial_\nu T^{i\nu} \hat{\mathbf{e}}_i \end{pmatrix} = \begin{pmatrix} \frac{1}{c} \left(\frac{\partial}{\partial t} W + \nabla \cdot \mathbf{\Pi} \right) \\ \frac{\partial}{\partial t} \mathbf{p} + \nabla \cdot \mathbf{T} \end{pmatrix} = 0, \quad (10)$$

where $W(t)$, $\mathbf{p}(t)$, $\mathbf{\Pi}(t)$ and $\mathbf{T}(t)$ are instantaneous energy and momentum densities, Poynting vector and Maxwell's stress tensor respectively. In the time-harmonic-time-averaged case, the time derivatives vanish. Equations (7) and (8), when compared to eq. (10), show that it is possible to define a tensor and pseudotensor that obey the continuity equation $\partial_\nu T^{\mu\nu} = 0$ as:

$$(T_0^{\mu\nu}) = \begin{pmatrix} W_0 & \omega\mathcal{S}_3 \\ c\mathbf{p}_0 & \mathbf{T}_0 \end{pmatrix}, \quad (T_3^{\mu\nu}) = \begin{pmatrix} W_3 & \omega\mathcal{S}_0 \\ c\mathbf{p}_3 & \mathbf{T}_3 \end{pmatrix}. \quad (11)$$

This illuminates the known fact that W_0 (energy) and W_3 (helicity) are densities of conserved quantities [2, 15, 39–42] whose flow is $\omega\mathcal{S}_3$ (\propto Poynting vector) and $\omega\mathcal{S}_0$ (\propto total spin), respectively (note the reversal $0 \leftrightarrow 3$), while $c\mathbf{p}_0$ (electromagnetic linear momentum density) and $c\mathbf{p}_3 = c(\mathbf{p}_R - \mathbf{p}_L)$ (chiral momentum) are conserved vector densities, with flow tensors \mathcal{T}_0 and \mathcal{T}_3 . Notice that $T_0^{\mu\nu} = T_R^{\mu\nu} + T_L^{\mu\nu}$ and $T_3^{\mu\nu} = T_R^{\mu\nu} - T_L^{\mu\nu}$ can be added or subtracted to get the energy-momentum tensors of the pure helicity components $T_{R/L}^{\mu\nu}$, such that

$$(T_{0/3}^{\mu\nu}) = \begin{pmatrix} W_R \pm W_L & \omega(\mathcal{S}_R \mp \mathcal{S}_L) \\ c(\mathbf{p}_R \pm \mathbf{p}_L) & \mathbf{T}_R \pm \mathbf{T}_L \end{pmatrix}. \quad (12)$$

This provides a relativistic framework for the quadratic quantities related to $A = 0, 3$, but leaves out the $A = 1, 2$ quantities. These do not admit a 4-tensor grouping. However, $W_1 = W_e - W_m$ and $W_2 = W_p - W_a$ are the time-average of the well-known relativistic electromagnetic invariants [43]:

$$\begin{aligned} W_1 &= \langle \varepsilon \|\mathcal{E}(t)\|^2 - \frac{1}{\mu} \|\mathcal{B}(t)\|^2 \rangle, \\ W_2 &= -\langle \frac{1}{\eta} \mathcal{B}(t) \cdot \mathcal{E}(t) \rangle, \end{aligned} \quad (13)$$

where $\mathcal{E}(t)$ and $\mathcal{H}(t)$ are the time-varying electric and magnetic fields. Hence, Lorentz boosts change both W_0 and W_3 , leaving $W_{1,2}$ unchanged. The normalised quantity W_3/W_0 is unchanged by Lorentz boosts, while $W_{1,2}/W_0$ change.

Interaction with matter — The different bases in the \mathbb{C}^2 space of (\mathbf{E}, \mathbf{H}) are associated with different symmetries, giving them a fundamental role in the interaction with symmetry-breaking matter. For instance, matter at optical frequencies has a predominantly electric response with negligible magnetism, breaking the EM symmetry and hence experiencing forces and torques related to $W_1 = W_e - W_m$, $\mathbf{p}_1 = \mathbf{p}_e - \mathbf{p}_m$, $\mathcal{S}_1 = \mathcal{S}_e - \mathcal{S}_m$. Chiral matter breaks RL symmetry, hence experiencing forces and torques [20] related to $W_3 = W_R - W_L$, \mathbf{p}_3 , \mathcal{S}_3 .

For small particles that scatter like an electric (\mathbf{p}) and a magnetic (\mathbf{m}) dipole, one can define the dipole moment bispinor $\boldsymbol{\pi}_{\text{EM}} = \frac{1}{2}(\mathbf{p}/\sqrt{\varepsilon}, \sqrt{\mu}\mathbf{m})^\top$ [10]. In analogy to the electromagnetic field bispinor $\boldsymbol{\psi}$ from eq. (1), this dipolar bispinor can be expressed in different bases such as $\boldsymbol{\pi}_{\text{PA}}$ and $\boldsymbol{\pi}_{\text{RL}}$. For linear response, dipole moments are proportional to applied fields, $\boldsymbol{\pi} = \mathbf{A}\boldsymbol{\psi}$, leading to a dipolar polarisability matrix \mathbf{A} which can too be expressed in the different bases (see supplementary). This notation simplifies many expressions on the interaction between light and dipolar particles. For example, the extinction power by a dipole under illumination $P_{\text{ext}} = \frac{\omega}{2}\Im(\mathbf{E}^* \cdot \mathbf{p} + \mu\mathbf{H}^* \cdot \mathbf{m})$ can be written using bispinors as $2\omega\Im(\boldsymbol{\psi}^\dagger \cdot \boldsymbol{\pi})$ and subsequently using the polarisability matrix via $2\omega\Im(\boldsymbol{\psi}^\dagger \cdot \mathbf{A}\boldsymbol{\psi})$ which, assuming isotropy, reduces (see supplementary) to the elegant \mathbb{C}^2 -basis-independent expression $P_{\text{ext}} = 2\omega(\Im\alpha_0 W_0 + \Im\alpha_1 W_1 + \Im\alpha_2 W_2 + \Im\alpha_3 W_3)$, where $\alpha_0 = \frac{1}{2}(\alpha_e + \alpha_m)$, $\alpha_1 = \frac{1}{2}(\alpha_e - \alpha_m)$, $\alpha_2 = \frac{1}{2}(\alpha_a - \alpha_p)$ (non-reciprocal polarisability) and $\alpha_3 = \frac{1}{2}(\alpha_R - \alpha_L)$ (chiral polarisability). Another example is the interaction force on a dipole $\mathbf{F} = \frac{1}{2}\Re\{\mathbf{p}^* \cdot (\nabla)\mathbf{E} + \mu\mathbf{m}^* \cdot (\nabla)\mathbf{H}\}$ which can be written [20] in a \mathbb{C}^2 -basis-independent way as $\mathbf{F} = \sum_{A=0}^3 (\Re[\alpha_A] \nabla W_A + 2\omega\Im[\alpha_A] \mathbf{p}_A)$, revealing gradient and pressure forces associated to each symmetry breaking. The fact that $W_1 = W_2 = 0$ in paraxial fields means that experiments with paraxial light will only access $\alpha_e + \alpha_m$ (total extinction spectra) and $\alpha_R - \alpha_L$ (optical activity and circular dichroism). Illumination with $W_1 \neq 0$ (such as an evanescent or standing wave) can be used to access α_1 and hence discern α_e from α_m .

The use of different bases for electromagnetic bispinors also provides insights into material response. The constitutive relations that define an isotropic linear material (allowing chirality and non-reciprocity) are traditionally written in the EM basis [44]:

$$\underbrace{\frac{1}{2} \begin{pmatrix} \mathbf{D}/\sqrt{\varepsilon_0} \\ \mathbf{B}/\sqrt{\mu_0} \end{pmatrix}}_{\boldsymbol{\gamma}_{\text{EM}}} = \underbrace{\begin{pmatrix} \underbrace{1 + \chi_e}_{\varepsilon_r} & \chi_t + i\chi_c \\ \chi_t - i\chi_c & \underbrace{1 + \chi_m}_{\mu_r} \end{pmatrix}}_{\mathbf{I} + \boldsymbol{\chi}_{\text{EM}}} \underbrace{\frac{1}{2} \begin{pmatrix} \sqrt{\varepsilon_0} \mathbf{E} \\ \sqrt{\mu_0} \mathbf{H} \end{pmatrix}}_{\boldsymbol{\psi}_{\text{EM}}}, \quad (14)$$

where χ_e is the electric susceptibility, $\varepsilon_r = 1 + \chi_e$ the relative electric permittivity, χ_m the magnetic susceptibility, $\mu_r = 1 + \chi_m$ the relative magnetic permeability, χ_c the chiral susceptibility (typically written as κ chiral material parameter in many works), and χ_t the non-reciprocal susceptibility. The constitutive relations motivate us to define a bispinor $\boldsymbol{\gamma}_{\text{EM}} = \frac{1}{2}(\mathbf{D}/\sqrt{\varepsilon_0}, \mathbf{B}/\sqrt{\mu_0})^\top$, which allows writing the constitutive relations in a basis-independent notation as $\boldsymbol{\gamma} = (\mathbf{I} + \boldsymbol{\chi})\boldsymbol{\psi}$. Under the lens of our framework, we propose the susceptibility tensor $\boldsymbol{\chi}$ may be written in the EM, PA, or RL basis (see supplementary) which motivates the use of four basis-independent material degrees of freedom, given by

$\chi_0 = \frac{1}{2}(\varepsilon_r + \mu_r) - 1 = \frac{1}{2}(\chi_e + \chi_m)$, and the differences $\chi_1 = \frac{1}{2}(\chi_e - \chi_m)$, $\chi_2 = -\chi_t = -\frac{1}{2}(\chi_p - \chi_a)$ and $\chi_3 = \chi_c = \frac{1}{2}(\chi_R - \chi_L)$. Additionally, as derived in the supplementary, the time-harmonic macroscopic Maxwell equations (in absence of free sources) can be written as:

$$\nabla \times \boldsymbol{\psi} = ik_0 \hat{D}\boldsymbol{\gamma}, \quad (15)$$

where the curl $\nabla \times = \begin{pmatrix} 0 & 0 \\ 0 & 1 \end{pmatrix} \nabla \times$ acts on the $\mathbb{C}^3 \times \mathbb{L}^3$ sub-space of bispinors, and \hat{D} represents the duality transformation acting on the \mathbb{C}^2 sub-space, given by $\hat{D}_{\text{EM}} = \begin{pmatrix} 0 & 1 \\ -1 & 0 \end{pmatrix}$ in the EM basis. Combining eqs. (14) and (15) one arrives at $[ik_0 \hat{D}(\mathbf{I} + \boldsymbol{\chi}) - \nabla \times] \boldsymbol{\psi} = 0$, which is of the form $\mathbf{M}\boldsymbol{\psi} = 0$. This has been done before in the EM basis, e.g. [45], but we here stress that the representation of \mathbf{M} depends on the \mathbb{C}^2 basis being used (see supplementary). This brings interesting insight. In the EM basis, the tensor \mathbf{M} and hence Maxwell's equations become diagonal (in \mathbb{C}^2) when $\varepsilon_r(\mathbf{r}) = 0$ and $\mu_r(\mathbf{r}) = 0$, which means that $\mathbf{F}_e(\mathbf{r})$ becomes uncoupled from $\mathbf{F}_m(\mathbf{r})$. Indeed, in such ε -and- μ -near-zero materials, it is known that Maxwell's equations become static-like and the electric and magnetic fields uncouple from each other [46, 47]. In the RL basis, diagonalisation of \mathbf{M} occurs under the condition $\varepsilon_r(\mathbf{r}) = \mu_r(\mathbf{r})$ and $\chi_t(\mathbf{r}) = 0$. It is known that in these so-called dual materials (free space being a trivial example), scattered light preserves the incident helicity [48], as $\mathbf{F}_R(\mathbf{r})$ is uncoupled from $\mathbf{F}_L(\mathbf{r})$. Finally, in the PA basis, diagonalisation occurs when $\varepsilon_r(\mathbf{r}) = -\mu_r(\mathbf{r})$ and $\chi_t(\mathbf{r}) = 0$, meaning $\mathbf{F}_p(\mathbf{r})$ and $\mathbf{F}_a(\mathbf{r})$ become uncoupled. This condition occurs in opaque plasmonic materials. We believe that further interesting insights in light-matter interactions can arise from this symmetry-based formalism.

Conclusions — By freeing ourselves from the electric-magnetic basis, and expressing electromagnetic fields in the parallel-antiparallel and right-left basis, a flood of insights and analogies is uncovered. By subtracting the energy and spin between field projections, a reinterpretation and systematization of known electromagnetic quadratic quantities and their relations results, in some cases leading to novel insights such as the wave-like behavior of the spin-like quantities. The symmetry sphere is a valuable resource to gain intuition and understanding of symmetry in electromagnetism and its interaction with matter, and we feel there is much room for its exploration. Our current analysis is limited to time-harmonic fields and quadratic quantities only, though we strongly believe the framework can be adapted to more general situations.

Acknowledgments — SG and FJRF acknowledge support from EIC-Pathfinder-CHIRALFORCE (101046961) which is funded by Innovate UK Horizon Europe Guarantee (UKRI project 10045438). AJV is supported by EPSRC Grant EP/R513064/1.

* sebastian.l.golat@kcl.ac.uk

† francisco.rodriguez.fortuno@kcl.ac.uk

- [1] R. P. Cameron, S. M. Barnett, and A. M. Yao, Optical helicity, optical spin and related quantities in electromagnetic theory, *New J. Phys.* **14**, 053050 (2012).
- [2] K. Y. Bliokh, A. Y. Bekshaev, and F. Nori, Dual electromagnetism: helicity, spin, momentum and angular momentum, *New J. Phys.* **15**, 033026 (2013).
- [3] A. Aiello and M. V. Berry, Note on the helicity decomposition of spin and orbital optical currents, *Journal of Optics* **17**, 062001 (2015).
- [4] S. M. Barnett, R. P. Cameron, and A. M. Yao, Duplex symmetry and its relation to the conservation of optical helicity, *Physical Review A* **86**, 013845 (2012).
- [5] K. Y. Bliokh and F. Nori, Characterizing optical chirality, *Physical Review A* **83**, 10.1103/PhysRevA.83.021803 (2011).
- [6] Y. Tang and A. E. Cohen, Optical chirality and its interaction with matter, *Physical Review Letters* **104**, 10.1103/PhysRevLett.104.163901 (2010).
- [7] A. J. Vernon, S. Golat, C. Rigouzzo, E. A. Lim, and F. J. Rodríguez-Fortuño, A decomposition of light's spin angular momentum density (2023), [arXiv:2310.03804](https://arxiv.org/abs/2310.03804) [physics.optics].
- [8] A. J. Vernon, M. R. Dennis, and F. J. Rodríguez-Fortuño, 3d zeros in electromagnetic fields, *Optica* **10**, 1231 (2023).
- [9] F. Alpeggiani, K. Y. Bliokh, F. Nori, and L. Kuipers, Electromagnetic helicity in complex media, *Phys. Rev. Lett.* **120**, 243605 (2018).
- [10] K. Y. Bliokh, Y. S. Kivshar, and F. Nori, Magnetoelectric effects in local light-matter interactions, *Phys. Rev. Lett.* **113**, 033601 (2014).
- [11] K. Y. Bliokh, A. Y. Bekshaev, and F. Nori, Extraordinary momentum and spin in evanescent waves, *Nature Communications* **5**, 10.1038/ncomms4300 (2014).
- [12] I. Białynicki-Birula, On the wave function of the photon, *Acta Physica Polonica A* **86**, 97–116 (1994).
- [13] I. Białynicki-Birula and Z. Białynicka-Birula, Vortex lines of the electromagnetic field, *Physical Review A* **67**, 062114 (2003).
- [14] G. Kaiser, Helicity, polarization and riemann–silberstein vortices, *Journal of Optics A: Pure and Applied Optics* **6**, S243–S245 (2004).
- [15] I. Fernandez-Corbaton, *Helicity and duality symmetry in light matter interactions: Theory and applications*, Ph.D. thesis, Macquarie University (2014).
- [16] J. L. Trueba and A. F. Rañada, The electromagnetic helicity, *European Journal of Physics* **17**, 141–144 (1996).
- [17] G. N. Afanasiev and Y. P. Stepanovsky, The helicity of the free electromagnetic field and its physical meaning, *Il Nuovo Cimento A* **109**, 271–279 (1996).
- [18] M. V. Berry and P. Shukla, Geometry of 3d monochromatic light: local wavevectors, phases, curl forces, and superoscillations, *Journal of Optics* **21**, 10.1088/2040-8986/ab14c4 (2019).
- [19] M. Nieto-Vesperinas and X. Xu, Reactive helicity and reactive power in nanoscale optics: Evanescent waves. kerker conditions. optical theorems and reactive dichroism, *Physical Review Research* **3**, 043080 (2021).
- [20] S. Golat, J. J. Kingsley-Smith, I. Diez, J. Martinez-Romeu, A. Martínez, and F. J. Rodríguez-Fortuño, Optical chiral sorting forces and their manifestation in evanescent waves and nanofibres (2023).
- [21] K. Y. Bliokh and F. Nori, Transverse spin of a surface polariton, *Physical Review A* **85**, 061801 (2012).
- [22] A. Aiello, P. Banzer, M. Neugebauer, and G. Leuchs, From transverse angular momentum to photonic wheels, *Nature Photonics* **9**, 789–795 (2015).
- [23] K. Y. Bliokh and F. Nori, Transverse and longitudinal angular momenta of light, *Physics Reports* **592**, 1–38 (2015).
- [24] K. Y. Bliokh, F. J. Rodríguez-Fortuño, F. Nori, and A. V. Zayats, Spin–orbit interactions of light, *Nature Photonics* **9**, 796–808 (2015).
- [25] A. Y. Bekshaev, K. Y. Bliokh, and F. Nori, Transverse spin and momentum in two-wave interference, *Physical Review X* **5**, 10.1103/PhysRevX.5.011039 (2015).
- [26] J. S. Eismann, L. H. Nicholls, D. J. Roth, M. A. Alonso, P. Banzer, F. J. Rodríguez-Fortuño, A. V. Zayats, F. Nori, and K. Y. Bliokh, Transverse spinning of unpolarized light, *Nature Photonics* **15**, 156–161 (2020).
- [27] L. Liu, A. D. Donato, V. Ginis, S. Kheifets, A. Amirzhan, and F. Capasso, Three-dimensional measurement of the helicity-dependent forces on a mie particle, *Physical Review Letters* **120**, 223901 (2018).
- [28] M. Antognozzi, C. R. Bermingham, R. L. Harniman, S. Simpson, J. Senior, R. Hayward, H. Hoerber, M. R. Dennis, A. Y. Bekshaev, K. Y. Bliokh, and F. Nori, Direct measurements of the extraordinary optical momentum and transverse spin-dependent force using a nanocantilever, *Nature Physics* **12**, 731–735 (2016).
- [29] L. Wei and F. J. Rodríguez-Fortuño, Momentum-space geometric structure of helical evanescent waves and its implications on near-field directionality, *Physical Review Applied* **13**, 014008 (2020).
- [30] L. Wei, A. V. Zayats, and F. J. Rodríguez-Fortuño, Interferometric evanescent wave excitation of a nanoantenna for ultrasensitive displacement and phase metrology, *Physical Review Letters* **121**, 193901 (2018).
- [31] L. Wei, M. F. Picardi, J. J. Kingsley-Smith, A. V. Zayats, and F. J. Rodríguez-Fortuño, Directional scattering from particles under evanescent wave illumination: the role of reactive power, *Optics Letters* **43**, 3393 (2018).
- [32] X. Xu and M. Nieto-Vesperinas, Azimuthal imaginary poynting momentum density, *Physical Review Letters* **123**, 233902 (2019).
- [33] Y. Zhou, X. Xu, Y. Zhang, M. Li, S. Yan, M. Nieto-Vesperinas, B. Li, C.-W. Qiu, and B. Yao, Observation of high-order imaginary poynting momentum optomechanics in structured light, *Proceedings of the National Academy of Sciences* **119**, 10.1073/pnas.2209721119 (2022).
- [34] F. J. Belinfante, On the current and the density of the electric charge, the energy, the linear momentum and the angular momentum of arbitrary fields, *Physica* **7**, 449–474 (1940).
- [35] M. V. Berry, Optical currents, *Journal of Optics A: Pure and Applied Optics* **11**, 10.1088/1464-4258/11/9/094001 (2009).
- [36] D. E. Soper, *Classical Field Theory* (Wiley, 1976).
- [37] P. Shi, L. Du, C. Li, A. V. Zayats, and X. Yuan, Transverse spin dynamics in structured electromagnetic guided waves, *Proceedings of the National Academy of Sciences*

- 118**, [10.1073/pnas.2018816118](https://doi.org/10.1073/pnas.2018816118) (2021).
- [38] A. Y. Bekshaev, Transverse spin and the hidden vorticity of propagating light fields, *Journal of the Optical Society of America A* **39**, 1577 (2022).
- [39] R. P. Cameron and S. M. Barnett, Electric–magnetic symmetry and noether's theorem, *New J. Phys.* **14**, 123019 (2012).
- [40] R. P. Cameron, S. M. Barnett, and A. M. Yao, Optical helicity of interfering waves, *Journal of Modern Optics* **61**, 25–31 (2014).
- [41] M. Nieto-Vesperinas, Optical theorem for the conservation of electromagnetic helicity: Significance for molecular energy transfer and enantiomeric discrimination by circular dichroism, *Physical Review A* **92**, 023813 (2015).
- [42] M. Nieto-Vesperinas, Optical torque: Electromagnetic spin and orbital-angular-momentum conservation laws and their significance, *Physical Review A* **92**, 043843 (2015).
- [43] L. D. Landau and E. M. Lifšic, *Course of theoretical physics*, 4th ed., Vol. Vol. 2 (Pergamon Press, Oxford [u.a.], 1994).
- [44] J. Mun, M. Kim, Y. Yang, T. Badloe, J. Ni, Y. Chen, C.-W. Qiu, and J. Rho, Electromagnetic chirality: from fundamentals to nontraditional chiroptical phenomena, *Light Sci. Appl.* **9**, [10.1038/s41377-020-00367-8](https://doi.org/10.1038/s41377-020-00367-8) (2020).
- [45] E. A. Muljarov and T. Weiss, Resonant-state expansion for open optical systems: generalization to magnetic, chiral, and bi-anisotropic materials, *Optics letters* **43**, 1978–1981 (2018).
- [46] R. W. Ziolkowski, Propagation in and scattering from a matched metamaterial having a zero index of refraction, *Physical Review E* **70**, 046608 (2004).
- [47] A. M. Mahmoud and N. Engheta, Wave–matter interactions in epsilon-and-mu-near-zero structures, *Nature communications* **5**, 5638 (2014).
- [48] X. Zambrana-Puyalto, I. Fernandez-Corbaton, M. Juan, X. Vidal, and G. Molina-Terriza, Duality symmetry and kerker conditions, *Optics letters* **38**, 1857–1859 (2013).

Supplementary Information for “The electromagnetic symmetry sphere: a framework for energy, momentum, spin and other electromagnetic quantities”

Sebastian Golat,^{*} Alex J. Vernon, and Francisco J. Rodríguez-Fortuño[†]
*Department of Physics, King’s College London, Strand, London WC2R 2LS, UK and
 London Centre for Nanotechnology*
 (Dated: May 27, 2024)

BISPINOR FORMALISM

Bases in the electromagnetic bispinor vector space

Electromagnetic bispinors are a mathematical description of electromagnetic fields. For monochromatic light, these bispinors live in a $\mathbb{C}^3 \times \mathbb{C}^2 \times \mathbb{L}^2(\mathbb{R}^3)$ vector space. The bispinor $\boldsymbol{\psi}(\mathbf{r})$ or $\boldsymbol{\psi}(\mathbf{k})$ contains all the information about the electromagnetic field at any point in real space \mathbf{r} or momentum space \mathbf{k} . Indeed it has the same information as the two complex phasor vectors \mathbf{E} and \mathbf{H} defined at a given point, hence most works write it as $\boldsymbol{\psi} = (\mathbf{E}, \mathbf{H})$, but this representation as a two-dimensional vector implicitly assumes a specific basis representation in the \mathbb{C}^2 space of electric and magnetic fields. Because we are going to choose different bases in that space, it is first convenient to re-scale our electric and magnetic field vectors in order to make their dimensions match and for them to be normalised in terms of energy. For this, consider the electromagnetic energy density in a linear, homogeneous, isotropic medium with permittivity ε and permeability μ :

$$W = \frac{1}{4}(\varepsilon|\mathbf{E}|^2 + \mu|\mathbf{H}|^2). \quad (1)$$

This expression suggests defining re-scaled vectors to describe electric and magnetic fields:

$$\begin{aligned} \mathbf{F}_e &\equiv \frac{1}{2}\sqrt{\varepsilon}\mathbf{E}, \\ \mathbf{F}_m &\equiv \frac{1}{2}\sqrt{\mu}\mathbf{H}, \end{aligned} \quad (2)$$

such that they have the same dimensions. The electromagnetic energy density can then be written as:

$$W = |\mathbf{F}_e|^2 + |\mathbf{F}_m|^2. \quad (3)$$

We can describe an electromagnetic field either with (\mathbf{E}, \mathbf{H}) vectors, or with $(\mathbf{F}_e, \mathbf{F}_m)$, knowing these two descriptions to be equivalent and differing only by fixed constants in a specific medium. Now let’s focus our attention on the $\mathbb{C}^3 \times \mathbb{C}^2$ nature of the electromagnetic bi-spinor (the remaining $\mathbb{L}^2(\mathbb{R}^3)$ nature describes the spatial or momentum space dependence of each field). The most common basis for this bi-spinor is to use $(\hat{\mathbf{x}}, \hat{\mathbf{y}}, \hat{\mathbf{z}})$ basis in the \mathbb{C}^3 space, and the electric-magnetic basis (let’s introduce unit vectors $(\hat{\mathbf{e}}, \hat{\mathbf{m}})$ to be defined later) in the \mathbb{C}^2 space, hence one can understand the bi-spinor as a six-dimensional entity composed of six scalar fields $\boldsymbol{\psi} = (F_{e,x}, F_{e,y}, F_{e,z}, F_{m,x}, F_{m,y}, F_{m,z})$ where $F_{e,x}$ is the x-component of \mathbf{F}_e , and so on. This can be understood as a linear combination of basis vectors as follows:

$$\boldsymbol{\psi} = F_{e,x}\hat{\mathbf{x}}\hat{\mathbf{e}} + F_{e,y}\hat{\mathbf{y}}\hat{\mathbf{e}} + F_{e,z}\hat{\mathbf{z}}\hat{\mathbf{e}} + F_{m,x}\hat{\mathbf{x}}\hat{\mathbf{m}} + F_{m,y}\hat{\mathbf{y}}\hat{\mathbf{m}} + F_{m,z}\hat{\mathbf{z}}\hat{\mathbf{m}} \quad (4)$$

where the product of unit vectors is an outer product between *different* vector spaces. We can factor out this expression in either of two ways:

$$\boldsymbol{\psi} = \psi_x\hat{\mathbf{x}} + \psi_y\hat{\mathbf{y}} + \psi_z\hat{\mathbf{z}} \quad \rightarrow \quad \psi_{[x,y,z]} = \underbrace{\psi_x}_{\mathbb{C}^2} \begin{pmatrix} 1 \\ 0 \\ 0 \end{pmatrix} + \underbrace{\psi_y}_{\mathbb{C}^2} \begin{pmatrix} 0 \\ 1 \\ 0 \end{pmatrix} + \underbrace{\psi_z}_{\mathbb{C}^2} \begin{pmatrix} 0 \\ 0 \\ 1 \end{pmatrix} = \begin{pmatrix} \psi_x \\ \psi_y \\ \psi_z \end{pmatrix}, \quad (5)$$

where $\psi_x = F_{e,x}\hat{\mathbf{e}} + F_{m,x}\hat{\mathbf{m}}$ is a \mathbb{C}^2 vector coefficient containing all information of electric and magnetic field’s x-components, and similarly for ψ_y and ψ_z . Alternatively, we can factor it as:

$$\boldsymbol{\psi} = \mathbf{F}_e \hat{\mathbf{e}} + \mathbf{F}_m \hat{\mathbf{m}} \quad \rightarrow \quad \boldsymbol{\psi}_{[\text{EM}]} = \underbrace{\mathbf{F}_e}_{\mathbb{C}^3} \underbrace{\begin{pmatrix} 1 \\ 0 \end{pmatrix}}_{\mathbb{C}^2} + \mathbf{F}_m \begin{pmatrix} 0 \\ 1 \end{pmatrix} = \begin{pmatrix} \mathbf{F}_e \\ \mathbf{F}_m \end{pmatrix} \quad (6)$$

where $\mathbf{F}_e = F_{e,x}\hat{\mathbf{x}} + F_{e,y}\hat{\mathbf{y}} + F_{e,z}\hat{\mathbf{z}}$ is a vector in \mathbb{C}^3 space that contains the information of the electric field in all spatial directions, and similarly for \mathbf{F}_m in the magnetic field.

The most unusual aspect of this notation for readers with an optics and electromagnetism background is that we are writing a linear combination of basis vectors in a given space, but the *coefficients* of this linear combination are themselves vectors in a different vector space. That is why $\boldsymbol{\psi}_{[\text{EM}]} = (\mathbf{F}_e, \mathbf{F}_m)$ is a vector (in \mathbb{C}^2) whose elements are themselves vectors (in \mathbb{C}^3). Also, when we write down vectors as an array of numbers, we are inherently defining a basis, as we just did for $\boldsymbol{\psi}_{[\text{EM}]}$, and we use square bracket subscript to explicitly indicate this. Alternatively, we may use linear combinations of basis vectors, such as $\boldsymbol{\psi} = \mathbf{F}_e \hat{\mathbf{e}} + \mathbf{F}_m \hat{\mathbf{m}}$ to keep a basis independent notation.

It is well known that the $(\hat{\mathbf{x}}, \hat{\mathbf{y}}, \hat{\mathbf{z}})$ basis is not the only basis to express three-dimensional vectors such as \mathbf{E} . Similarly, and this being the key point of this manuscript, the electric-magnetic $(\hat{\mathbf{e}}, \hat{\mathbf{m}})$ basis used in \mathbb{C}^2 subspace in eq. (6) is not the only basis in that space. In fact, being a \mathbb{C}^2 space isomorphic with the Jones vectors of the field in a plane, we take inspiration on the horizontal-vertical, diagonal-antidiagonal, and right-left-handed polarisation bases, to define the following unit vectors:

$$\begin{aligned} \hat{\mathbf{p}} &= (\hat{\mathbf{e}} + \hat{\mathbf{m}})/\sqrt{2}, & \hat{\mathbf{r}} &= (\hat{\mathbf{e}} + i\hat{\mathbf{m}})/\sqrt{2}, \\ \hat{\mathbf{a}} &= (\hat{\mathbf{e}} - \hat{\mathbf{m}})/\sqrt{2}, & \hat{\mathbf{l}} &= (\hat{\mathbf{e}} - i\hat{\mathbf{m}})/\sqrt{2}. \end{aligned} \quad (7)$$

These basis vectors form three orthonormal bases in the \mathbb{C}^2 subspace of $\boldsymbol{\psi}$: the EM basis $(\hat{\mathbf{e}}, \hat{\mathbf{m}})$ distinguishing electric and magnetic fields, the PA basis $(\hat{\mathbf{p}}, \hat{\mathbf{a}})$ distinguishing between states where electric and magnetic fields are parallel or antiparallel, and the RL basis $(\hat{\mathbf{r}}, \hat{\mathbf{l}})$ which corresponds to distinguishing fields with different helicities. These three bases are depicted in the main text Fig. 1. Any electromagnetic field $\boldsymbol{\psi}$ can be written as a linear combination in any of these bases:

$$\boxed{\boldsymbol{\psi} = \mathbf{F}_e \hat{\mathbf{e}} + \mathbf{F}_m \hat{\mathbf{m}} = \mathbf{F}_p \hat{\mathbf{p}} + \mathbf{F}_a \hat{\mathbf{a}} = \mathbf{F}_R \hat{\mathbf{r}} + \mathbf{F}_L \hat{\mathbf{l}}} \quad (8)$$

where the coefficients \mathbf{F}_i are vectors in \mathbb{C}^3 . This implies that we may write this bispinor as an array of two elements by choosing different bases, resulting in the notation:

$$\boldsymbol{\psi}_{[\text{EM}]} = \begin{pmatrix} \mathbf{F}_e \\ \mathbf{F}_m \end{pmatrix} \quad \boldsymbol{\psi}_{[\text{PA}]} = \begin{pmatrix} \mathbf{F}_p \\ \mathbf{F}_a \end{pmatrix} \quad \boldsymbol{\psi}_{[\text{RL}]} = \begin{pmatrix} \mathbf{F}_R \\ \mathbf{F}_L \end{pmatrix}, \quad (9)$$

as used in Eq. (1) in the main text. The unit vectors are normalised such that they each correspond to electromagnetic fields with unit energy density. We can conclude that electromagnetic energy density from eq. (3) is the norm of the electromagnetic bispinor, and thus thanks to Parseval's theorem can be written in terms of the coefficients in any basis:

$$W = \|\boldsymbol{\psi}\|^2 = |\mathbf{F}_e|^2 + |\mathbf{F}_m|^2 = |\mathbf{F}_p|^2 + |\mathbf{F}_a|^2 = |\mathbf{F}_R|^2 + |\mathbf{F}_L|^2. \quad (10)$$

For completeness and clarity, the simultaneous eq. (8) can be written explicitly in each basis:

$$\begin{aligned} \boldsymbol{\psi}_{[\text{EM}]} &= \begin{pmatrix} \mathbf{F}_e \\ \mathbf{F}_m \end{pmatrix} = \mathbf{F}_e \begin{pmatrix} 1 \\ 0 \end{pmatrix} + \mathbf{F}_m \begin{pmatrix} 0 \\ 1 \end{pmatrix} = \mathbf{F}_p \begin{pmatrix} \frac{1}{\sqrt{2}} \\ \frac{1}{\sqrt{2}} \end{pmatrix} + \mathbf{F}_a \begin{pmatrix} \frac{1}{\sqrt{2}} \\ -\frac{1}{\sqrt{2}} \end{pmatrix} = \mathbf{F}_R \begin{pmatrix} \frac{1}{\sqrt{2}} \\ i \end{pmatrix} + \mathbf{F}_L \begin{pmatrix} \frac{1}{\sqrt{2}} \\ -i \end{pmatrix} \\ \boldsymbol{\psi}_{[\text{PA}]} &= \begin{pmatrix} \mathbf{F}_p \\ \mathbf{F}_a \end{pmatrix} = \mathbf{F}_e \begin{pmatrix} \frac{1}{\sqrt{2}} \\ \frac{1}{\sqrt{2}} \end{pmatrix} + \mathbf{F}_m \begin{pmatrix} \frac{1}{\sqrt{2}} \\ -\frac{1}{\sqrt{2}} \end{pmatrix} = \mathbf{F}_p \begin{pmatrix} 1 \\ 0 \end{pmatrix} + \mathbf{F}_a \begin{pmatrix} 0 \\ 1 \end{pmatrix} = \mathbf{F}_R \begin{pmatrix} \frac{1+i}{2} \\ \frac{1-i}{2} \end{pmatrix} + \mathbf{F}_L \begin{pmatrix} \frac{1-i}{2} \\ \frac{1+i}{2} \end{pmatrix} \\ \boldsymbol{\psi}_{[\text{RL}]} &= \begin{pmatrix} \mathbf{F}_R \\ \mathbf{F}_L \end{pmatrix} = \underbrace{\mathbf{F}_e}_{\hat{\mathbf{e}}} \underbrace{\begin{pmatrix} \frac{1}{\sqrt{2}} \\ \frac{1}{\sqrt{2}} \end{pmatrix}}_{\hat{\mathbf{m}}} + \mathbf{F}_m \underbrace{\begin{pmatrix} \frac{-i}{\sqrt{2}} \\ \frac{i}{\sqrt{2}} \end{pmatrix}}_{\hat{\mathbf{m}}} = \mathbf{F}_p \underbrace{\begin{pmatrix} \frac{1-i}{2} \\ \frac{1+i}{2} \end{pmatrix}}_{\hat{\mathbf{p}}} + \mathbf{F}_a \underbrace{\begin{pmatrix} \frac{1+i}{2} \\ \frac{1-i}{2} \end{pmatrix}}_{\hat{\mathbf{a}}} = \mathbf{F}_R \underbrace{\begin{pmatrix} 1 \\ 0 \end{pmatrix}}_{\hat{\mathbf{r}}} + \mathbf{F}_L \underbrace{\begin{pmatrix} 0 \\ 1 \end{pmatrix}}_{\hat{\mathbf{l}}} \end{aligned} \quad (11)$$

where we have expressed each of the six basis vectors using each of the three orthonormal bases, by re-arranging eq. (7), revealing the strict relations between the different \mathbf{F}_i .

This completes the formal description of our approach to the different bases for electromagnetic bi-spinors. It is however interesting to also consider how this approach translates into the usual language of \mathbf{E} and \mathbf{H} as we do in the next section.

Bispinor basis formalism in terms of \mathbf{E} and \mathbf{H}

Basis name	$\mathbf{F}[\mathbb{C}^3] \otimes \hat{\mathbf{u}}[\mathbb{C}^2]$	Meaning in terms of \mathbf{E} and \mathbf{H}
EM basis	$\mathbf{F}_e \hat{\mathbf{e}}$ $\mathbf{F}_m \hat{\mathbf{m}}$	$\mathbf{E} = 2\mathbf{F}_e/\sqrt{\varepsilon}$ and $\mathbf{H} = \mathbf{0}$ $\mathbf{E} = \mathbf{0}$ and $\mathbf{H} = 2\mathbf{F}_m/\sqrt{\mu}$
PA basis	$\mathbf{F}_p \hat{\mathbf{p}}$ $\mathbf{F}_a \hat{\mathbf{a}}$	$\mathbf{E} = \sqrt{2}\mathbf{F}_p/\sqrt{\varepsilon}$ and $\mathbf{H} = \sqrt{2}\mathbf{F}_p/\sqrt{\mu}$ $\mathbf{E} = \sqrt{2}\mathbf{F}_a/\sqrt{\varepsilon}$ and $\mathbf{H} = -\sqrt{2}\mathbf{F}_a/\sqrt{\mu}$
RL basis	$\mathbf{F}_R \hat{\mathbf{r}}$ $\mathbf{F}_L \hat{\mathbf{l}}$	$\mathbf{E} = \sqrt{2}\mathbf{F}_R/\sqrt{\varepsilon}$ and $\mathbf{H} = i\sqrt{2}\mathbf{F}_R/\sqrt{\mu}$ $\mathbf{E} = \sqrt{2}\mathbf{F}_L/\sqrt{\varepsilon}$ and $\mathbf{H} = -i\sqrt{2}\mathbf{F}_L/\sqrt{\mu}$

TABLE I. The precise meaning of the \mathbb{C}^2 basis vectors in terms of \mathbf{E} and \mathbf{H} . To derive this table, start by the definitions in eq. (2) to find the first row, and then use the definitions in eq. (7) to evaluate the other rows.

In table I we write down what each \mathbb{C}^2 basis vector, when multiplied by a \mathbb{C}^3 vector \mathbf{F} , implies in terms of electric and magnetic fields. Using table I we can expand the simultaneous linear combinations in eq. (8) into its electric and magnetic counterparts:

$$\begin{aligned} \mathbf{E} &= \frac{2}{\sqrt{\varepsilon}}(\mathbf{F}_e + \mathbf{0}) = \frac{\sqrt{2}}{\sqrt{\varepsilon}}(\mathbf{F}_p + \mathbf{F}_a) = \frac{\sqrt{2}}{\sqrt{\varepsilon}}(\mathbf{F}_R + \mathbf{F}_L), \\ \mathbf{H} &= \frac{2}{\sqrt{\mu}}(\mathbf{0} + \mathbf{F}_m) = \frac{\sqrt{2}}{\sqrt{\mu}}(\mathbf{F}_p - \mathbf{F}_a) = \frac{\sqrt{2}}{\sqrt{\mu}}(i\mathbf{F}_R - i\mathbf{F}_L). \end{aligned} \quad (12)$$

which we may rewrite by defining vector fields \mathbf{E}_i and \mathbf{H}_i with $i = \{e, m, p, a, R, L\}$ in a way that highlights the decomposition of electromagnetic fields into the sum of the projections on each basis:

$$\begin{aligned} \mathbf{E} &= \mathbf{E}_e + \mathbf{E}_m = \mathbf{E}_p + \mathbf{E}_a = \mathbf{E}_R + \mathbf{E}_L, \\ \mathbf{H} &= \mathbf{H}_e + \mathbf{H}_m = \mathbf{H}_p + \mathbf{H}_a = \mathbf{H}_R + \mathbf{H}_L. \end{aligned} \quad (13)$$

Now, eq. (12) can be inverted to write the coefficients \mathbf{F}_i in terms of \mathbf{E} and \mathbf{H} :

$$\begin{aligned} \mathbf{F}_e &= \frac{1}{2}\sqrt{\varepsilon}\mathbf{E}, & \mathbf{F}_p &= \frac{1}{2\sqrt{2}}(\sqrt{\varepsilon}\mathbf{E} + \sqrt{\mu}\mathbf{H}), & \mathbf{F}_R &= \frac{1}{2\sqrt{2}}(\sqrt{\varepsilon}\mathbf{E} + i\sqrt{\mu}\mathbf{H}) \\ \mathbf{F}_m &= \frac{1}{2}\sqrt{\mu}\mathbf{H}, & \mathbf{F}_a &= \frac{1}{2\sqrt{2}}(\sqrt{\varepsilon}\mathbf{E} - \sqrt{\mu}\mathbf{H}), & \mathbf{F}_L &= \frac{1}{2\sqrt{2}}(\sqrt{\varepsilon}\mathbf{E} - i\sqrt{\mu}\mathbf{H}). \end{aligned} \quad (14)$$

Combining eqs. (9) and (14) we arrive at Eq. 1 in the main text, reproduced here:

$$\begin{aligned} \psi_{[\text{EM}]}(\mathbf{r}) &= \begin{pmatrix} \mathbf{F}_e \\ \mathbf{F}_m \end{pmatrix} = \frac{1}{2} \begin{pmatrix} \sqrt{\varepsilon}\mathbf{E} \\ \sqrt{\mu}\mathbf{H} \end{pmatrix}, \\ \psi_{[\text{PA}]}(\mathbf{r}) &= \begin{pmatrix} \mathbf{F}_p \\ \mathbf{F}_a \end{pmatrix} = \frac{1}{2\sqrt{2}} \begin{pmatrix} \sqrt{\varepsilon}\mathbf{E} + \sqrt{\mu}\mathbf{H} \\ \sqrt{\varepsilon}\mathbf{E} - \sqrt{\mu}\mathbf{H} \end{pmatrix}, \\ \psi_{[\text{RL}]}(\mathbf{r}) &= \begin{pmatrix} \mathbf{F}_R \\ \mathbf{F}_L \end{pmatrix} = \frac{1}{2\sqrt{2}} \begin{pmatrix} \sqrt{\varepsilon}\mathbf{E} + i\sqrt{\mu}\mathbf{H} \\ \sqrt{\varepsilon}\mathbf{E} - i\sqrt{\mu}\mathbf{H} \end{pmatrix}. \end{aligned} \quad (15)$$

And combining eqs. (12) to (14) we arrive at Eq. 3 from the main text, reproduced here:

$$\begin{aligned} \mathbf{E} &= \mathbf{E}_e + \mathbf{E}_m = \mathbf{E} + \mathbf{0} \\ &= \mathbf{E}_p + \mathbf{E}_a = \frac{\mathbf{E} + \eta\mathbf{H}}{2} + \frac{\mathbf{E} - \eta\mathbf{H}}{2} \\ &= \mathbf{E}_R + \mathbf{E}_L = \frac{\mathbf{E} + i\eta\mathbf{H}}{2} + \frac{\mathbf{E} - i\eta\mathbf{H}}{2} \end{aligned} \quad (16)$$

with the corresponding $\mathbf{H}_e = \mathbf{0}$, $\mathbf{H}_m = \mathbf{H}$, $\mathbf{H}_{p,a} = \pm\mathbf{E}_{p,a}/\eta$ and $\mathbf{H}_{R,L} = \mp i\mathbf{E}_{R,L}/\eta$, and $\eta = \sqrt{\mu/\varepsilon}$. Equation (16) provides a recipe for directly splitting any electromagnetic field (\mathbf{E} , \mathbf{H}) into a mathematical sum of two projections into the two basis vectors of any of the basis EM, PA or RL.

Microscopic Maxwell's equations in different bases

The use of different bases to describe electromagnetic fields is theoretically on the same footing as the traditional \mathbf{E} and \mathbf{H} approach. In fact, one can rewrite Maxwell's equations using them, and the well-known duality symmetry of Maxwell's equations makes them particularly pleasant. Following standard notation with ρ being charge density and \mathbf{J} being current density, the dual symmetric (including magnetic charges and currents) microscopic Maxwell's equations for time-harmonic fields are

$$\begin{aligned}\nabla \cdot \sqrt{\varepsilon} \mathbf{E} &= \rho_e / \sqrt{\varepsilon}, \\ \nabla \cdot \sqrt{\mu} \mathbf{H} &= \rho_m / \sqrt{\mu}, \\ \nabla \times \sqrt{\varepsilon} \mathbf{E} &= +ik\sqrt{\mu} \mathbf{H} - \sqrt{\varepsilon} \mathbf{J}_m, \\ \nabla \times \sqrt{\mu} \mathbf{H} &= -ik\sqrt{\varepsilon} \mathbf{E} + \sqrt{\mu} \mathbf{J}_e.\end{aligned}\tag{17}$$

These can be rewritten in terms of the basis coefficients \mathbf{F}_i where $i \in \{e, m, p, a, R, L\}$. In order to do that we need to find what charge and current densities look in those different bases. We may define the following scaled versions of charge and current densities:

$$\begin{aligned}f_e &= \frac{\rho_e}{2\sqrt{\varepsilon}}, & \mathbf{g}_e &= \frac{\mathbf{J}_e}{2c\sqrt{\varepsilon}}, \\ f_m &= \frac{\rho_m}{2\sqrt{\mu}}, & \mathbf{g}_m &= \frac{\mathbf{J}_m}{2c\sqrt{\mu}},\end{aligned}\tag{18}$$

such that, $\mathbf{F}_e = \sqrt{\varepsilon} \mathbf{E} / 2$ and $\mathbf{F}_m = \sqrt{\mu} \mathbf{H} / 2$ constitute a simple re-scaling of Maxwell's equations,

$$\begin{aligned}\nabla \cdot \mathbf{F}_{e/m} &= f_{e/m}, \\ \nabla \times \mathbf{F}_{e/m} &= \pm [ik\mathbf{F}_{m/e} - \mathbf{g}_{m/e}].\end{aligned}\tag{19}$$

Next, to get the equations in the right-left basis we need to combine them to get fields $\mathbf{F}_{R/L} = (\mathbf{F}_e \pm i\mathbf{F}_m) / \sqrt{2}$, which will lead to charge and current density combinations: $f_{R/L} = (f_e \pm if_m) / \sqrt{2}$ and $\mathbf{g}_{R/L} = (\mathbf{g}_e \pm i\mathbf{g}_m) / \sqrt{2}$, leading to

$$\begin{aligned}\nabla \cdot \mathbf{F}_{R/L} &= f_{R/L}, \\ \nabla \times \mathbf{F}_{R/L} &= \pm [k\mathbf{F}_{R/L} + i\mathbf{g}_{R/L}].\end{aligned}\tag{20}$$

Note that in this basis the right and left fields don't mix, unlike in the usual electromagnetic basis. To obtain Maxwell's equations in the parallel-antiparallel basis, we need the fields to be $\mathbf{F}_{p/a} = (\mathbf{F}_e \pm \mathbf{F}_m) / \sqrt{2}$, charge densities to be $f_{p/a} = (f_e \pm f_m) / \sqrt{2}$, and current densities $\mathbf{g}_{p/a} = (\mathbf{g}_e \pm \mathbf{g}_m) / \sqrt{2}$. These combinations yield

$$\begin{aligned}\nabla \cdot \mathbf{F}_{p/a} &= f_{p/a}, \\ \nabla \times \mathbf{F}_{p/a} &= \mp [ik\mathbf{F}_{a/p} - \mathbf{g}_{a/p}].\end{aligned}\tag{21}$$

Of course, these are just some arbitrary choices of bases in \mathbb{C}^2 and we could make a different choice (take a different linear combination of Maxwell's equations), however, one can define a charge density in the $\mathbb{C}^2 \times \mathbb{L}^2(\mathbb{R}^3)$ vector space as

$$\mathbf{f} = f_e \hat{\mathbf{e}} + f_m \hat{\mathbf{m}} = f_p \hat{\mathbf{p}} + f_a \hat{\mathbf{a}} = f_R \hat{\mathbf{r}} + f_L \hat{\mathbf{l}}\tag{22}$$

and a current bispinor in the $\mathbb{C}^3 \times \mathbb{C}^2 \times \mathbb{L}^2(\mathbb{R}^3)$ vector space as

$$\mathbf{g} = \mathbf{g}_e \hat{\mathbf{e}} + \mathbf{g}_m \hat{\mathbf{m}} = \mathbf{g}_p \hat{\mathbf{p}} + \mathbf{g}_a \hat{\mathbf{a}} = \mathbf{g}_R \hat{\mathbf{r}} + \mathbf{g}_L \hat{\mathbf{l}}\tag{23}$$

to write the time-harmonic microscopic Maxwell's equations in a basis-independent manner as

$$\begin{aligned}\nabla \cdot \psi &= \mathbf{f}, \\ \nabla \times \psi &= \hat{D}(ik\psi - \mathbf{g}),\end{aligned}\tag{24}$$

where \hat{D} is the electromagnetic duality transformation $\hat{D}\hat{\mathbf{e}} = \hat{\mathbf{m}}$ and $\hat{D}\hat{\mathbf{m}} = -\hat{\mathbf{e}}$.

QUADRATIC QUANTITIES AND SYMMETRY SPHERE

Linear transformations in \mathbb{C}^2 sub-space written in different bases

Any linear transformation \mathbf{A} in the \mathbb{C}^2 subspace can be represented, in any given basis, as a 2×2 matrix:

$$\mathbf{A} = \begin{pmatrix} a_{11} & a_{12} \\ a_{21} & a_{22} \end{pmatrix}. \quad (25)$$

Such a transformation has four complex degrees of freedom embodied by the four scalars a_{ij} . It is well-known that any such transformation can be written as a linear combination of four matrices that form a complete basis in this space: the identity matrix I , and the three Pauli matrices $\sigma_{1,2,3}$, with complex coefficients $a_{0,1,2,3}$ being the four equivalent degrees of freedom:

$$\begin{pmatrix} a_{11} & a_{12} \\ a_{21} & a_{22} \end{pmatrix} = a_0 \underbrace{\begin{pmatrix} 1 & 0 \\ 0 & 1 \end{pmatrix}}_I + a_1 \underbrace{\begin{pmatrix} 0 & 1 \\ 1 & 0 \end{pmatrix}}_{\sigma_1} + a_2 \underbrace{\begin{pmatrix} 0 & -i \\ i & 0 \end{pmatrix}}_{\sigma_2} + a_3 \underbrace{\begin{pmatrix} 1 & 0 \\ 0 & -1 \end{pmatrix}}_{\sigma_3} = \begin{pmatrix} a_0 + a_1 & a_3 - ia_2 \\ a_3 + ia_2 & a_0 - a_1 \end{pmatrix}, \quad (26)$$

from where we can obtain the determinant $\det(\mathbf{A}) = a_{11}a_{22} - a_{12}a_{21} = a_0^2 - a_1^2 - a_2^2 - a_3^2$. Equation (26) enables writing any transformation in a basis-independent way, via the four coefficients, as:

$$\mathbf{A} = a_0 \mathbf{W}_0 + a_1 \mathbf{W}_1 + a_2 \mathbf{W}_2 + a_3 \mathbf{W}_3. \quad (27)$$

This is extremely useful. Because the Pauli matrices swap into one another when changing between the \mathbb{C}^2 bases (using change of basis matrices and similarity transformations, which we won't review here), this notation allows us to easily change the basis for any arbitrary linear transformation, preserving the same set of four coefficients $a_{0,1,2,3}$, only requiring using the appropriate Pauli matrix, and with the correct sign, in place of each \mathbf{W}_i :

	\mathbf{W}_0	\mathbf{W}_1	\mathbf{W}_2	\mathbf{W}_3
RL basis	I	σ_1	σ_2	σ_3
EM basis	I	σ_3	$-\sigma_1$	$-\sigma_2$
PA basis	I	σ_1	$-\sigma_3$	σ_2
transformation	1	$-\hat{P}$	$\hat{P}\hat{D}$	$i\hat{D}$

TABLE II. Changing the basis of linear transformations in \mathbb{C}^2 .

For completeness and clarity, we write here how any arbitrary linear transformation would be written in each of the three bases:

$$\begin{aligned} \mathbf{A}_{[\text{RL}]} &= \begin{pmatrix} a_{\text{R}} & a_{\text{RL}} \\ a_{\text{LR}} & a_{\text{L}} \end{pmatrix} = a_0 \begin{pmatrix} 1 & 0 \\ 0 & 1 \end{pmatrix} + a_1 \underbrace{\begin{pmatrix} 0 & 1 \\ 1 & 0 \end{pmatrix}}_{\sigma_1} + a_2 \underbrace{\begin{pmatrix} 0 & -i \\ i & 0 \end{pmatrix}}_{\sigma_2} + a_3 \underbrace{\begin{pmatrix} 1 & 0 \\ 0 & -1 \end{pmatrix}}_{\sigma_3}, \\ \mathbf{A}_{[\text{EM}]} &= \begin{pmatrix} a_{\text{e}} & a_{\text{em}} \\ a_{\text{me}} & a_{\text{m}} \end{pmatrix} = a_0 \begin{pmatrix} 1 & 0 \\ 0 & 1 \end{pmatrix} + a_1 \underbrace{\begin{pmatrix} 1 & 0 \\ 0 & -1 \end{pmatrix}}_{\sigma_3} - a_2 \underbrace{\begin{pmatrix} 0 & 1 \\ 1 & 0 \end{pmatrix}}_{\sigma_1} - a_3 \underbrace{\begin{pmatrix} 0 & -i \\ i & 0 \end{pmatrix}}_{\sigma_2}, \\ \mathbf{A}_{[\text{PA}]} &= \begin{pmatrix} a_{\text{p}} & a_{\text{pa}} \\ a_{\text{ap}} & a_{\text{a}} \end{pmatrix} = a_0 \begin{pmatrix} 1 & 0 \\ 0 & 1 \end{pmatrix} + a_1 \underbrace{\begin{pmatrix} 0 & 1 \\ 1 & 0 \end{pmatrix}}_{\sigma_1} - a_2 \underbrace{\begin{pmatrix} 1 & 0 \\ 0 & -1 \end{pmatrix}}_{\sigma_3} + a_3 \underbrace{\begin{pmatrix} 0 & -i \\ i & 0 \end{pmatrix}}_{\sigma_2}, \end{aligned} \quad (28)$$

which provides a nice interpretation for the meaning of the coefficients:

$$\begin{aligned} a_0 &= \frac{1}{2}(a_{\text{R}} + a_{\text{L}}) = \frac{1}{2}(a_{\text{e}} + a_{\text{m}}) = \frac{1}{2}(a_{\text{p}} + a_{\text{a}}), \\ a_1 &= \frac{1}{2}(a_{\text{e}} - a_{\text{m}}), \\ a_2 &= -\frac{1}{2}(a_{\text{p}} - a_{\text{a}}), \\ a_3 &= \frac{1}{2}(a_{\text{R}} - a_{\text{L}}). \end{aligned} \quad (29)$$

The three matrix representations $\mathbf{A}_{[\text{RL}]}$, $\mathbf{A}_{[\text{EM}]}$ and $\mathbf{A}_{[\text{PA}]}$ are *similar matrices* in the mathematical sense, as they represent the same linear transformation in different bases, and therefore they all have the same trace and determinant:

$$\begin{aligned}\text{tr } \mathbf{A} &= 2a_0, \\ \det \mathbf{A} &= a_0^2 - a_1^2 - a_2^2 - a_3^2.\end{aligned}\tag{30}$$

We made a choice of matching the subscript i of the basis-independent tensor \mathbf{W}_i and its coefficient a_i to the number of the corresponding Pauli matrix $\boldsymbol{\sigma}_i$ for the RL basis. This arbitrary choice was taken after some consideration, such that the numbering 0, 1, 2, 3 matches the Stokes parameters when calculating the different energies in the main text. This arbitrary choice, which we carefully considered, has some consequences in other definitions. For example, $W_2 = -(W_p - W_a)$ with a negative sign, because eq. (28) has a negative sign in the coefficient of $\begin{pmatrix} 1 & 0 \\ 0 & -1 \end{pmatrix}$ for the PA basis. Similarly, in a later definition of material susceptibility, eq. (71), we have $\chi_2 = -\chi_t = -(\chi_p - \chi_a)/2$, with again a negative sign, due to this choice.

Stokes parameters and the Poincaré sphere

As mentioned before the \mathbb{C}^2 subspace of electromagnetic bispinors is analogous to the Jones vectors. Any polarised paraxial light can be represented by a \mathbb{C}^2 vector \mathbf{J} such that the electric field phasor can be written as

$$\sqrt{\varepsilon}\mathbf{E} = (\mathbf{J}^\top \hat{\mathbf{e}})e^{ikz} = (A_h \ A_v) \begin{pmatrix} \hat{\mathbf{e}}_h \\ \hat{\mathbf{e}}_v \end{pmatrix} e^{ikz} = (A_d \ A_a) \begin{pmatrix} \hat{\mathbf{e}}_d \\ \hat{\mathbf{e}}_a \end{pmatrix} e^{ikz} = (A_R \ A_L) \begin{pmatrix} \hat{\mathbf{e}}_R \\ \hat{\mathbf{e}}_L \end{pmatrix} e^{ikz},\tag{31}$$

where (A_h, A_v) are linear horizontal-vertical, (A_d, A_a) diagonal-antidiagonal and (A_R, A_L) right-left circular polarisation complex amplitudes. The outer product of the Jones vector with itself produces a tensor which, following eq. (26), may be written as a linear combination of Pauli matrices, whose coefficients are one half of the Stokes parameters as they are conventionally defined

$$\mathbf{J}\mathbf{J}_{[\text{ps}]}^\dagger = \begin{pmatrix} A_h \\ A_v \end{pmatrix} \begin{pmatrix} A_h^* & A_v^* \end{pmatrix} = \begin{pmatrix} |A_h|^2 & A_h A_v^* \\ A_v A_h^* & |A_v|^2 \end{pmatrix} = \frac{1}{2} \begin{pmatrix} \mathcal{S}_0 + \mathcal{S}_1 & \mathcal{S}_2 - i\mathcal{S}_3 \\ \mathcal{S}_2 + i\mathcal{S}_3 & \mathcal{S}_0 - \mathcal{S}_1 \end{pmatrix}, \quad (\text{linear basis})\tag{32}$$

and similarly in the diagonal-antidiagonal and right-left circular bases. Following eq. (29) one can express the Stokes parameters as they are most well-known:

$$\begin{aligned}\mathcal{S}_0 &= |A_h|^2 + |A_v|^2 = |A_d|^2 + |A_a|^2 = |A_R|^2 + |A_L|^2, \\ \mathcal{S}_1 &= |A_h|^2 - |A_v|^2, \\ \mathcal{S}_2 &= |A_d|^2 - |A_a|^2, \\ \mathcal{S}_3 &= |A_R|^2 - |A_L|^2.\end{aligned}\tag{33}$$

One can easily see that $\det \mathbf{J}\mathbf{J}^\dagger = |A_h|^2 |A_v|^2 - |A_h A_v^*|^2 = 0$ which, following eq. (30), leads to $\mathcal{S}_0^2 = \mathcal{S}_1^2 + \mathcal{S}_2^2 + \mathcal{S}_3^2$ (with the equality becoming an inequality for partially-polarised or unpolarised fields). This justifies why every polarisation state, characterised by coordinates $(\mathcal{S}_1, \mathcal{S}_2, \mathcal{S}_3)$, is contained in a Poincaré sphere with radius \mathcal{S}_0 . In the next section we will show that the \mathbb{C}^2 subspace of electromagnetic bispinors gives us exactly the same structure.

Energy and the symmetry sphere

According to eq. (10) the electromagnetic energy density is given by the inner product of the electromagnetic bispinor with itself:

$$\begin{aligned}W &= \boldsymbol{\psi}^\dagger \cdot \boldsymbol{\psi} = \|\boldsymbol{\psi}\|^2 && (\text{basis-independent notation}) \\ W_{[\text{EM}]} &= (\mathbf{F}_e^* \ \mathbf{F}_m^*) \cdot \begin{pmatrix} \mathbf{F}_e \\ \mathbf{F}_m \end{pmatrix} = \mathbf{F}_e^* \cdot \mathbf{F}_e + \mathbf{F}_m^* \cdot \mathbf{F}_m = W_e + W_m && (\text{EM basis})\end{aligned}\tag{34}$$

The outer product (in \mathbb{C}^2 space) of the electromagnetic bi-spinor with itself produces a tensor:

$$\begin{aligned} \mathbf{W} &= \boldsymbol{\psi} \cdot \boldsymbol{\psi}^\dagger && \text{(basis-independent notation)} \\ \mathbf{W}_{[\text{EM}]} &= \begin{pmatrix} \mathbf{F}_e \\ \mathbf{F}_m \end{pmatrix} \cdot \begin{pmatrix} \mathbf{F}_e^* & \mathbf{F}_m^* \end{pmatrix} = \begin{pmatrix} \mathbf{F}_e \cdot \mathbf{F}_e^* & \mathbf{F}_e \cdot \mathbf{F}_m^* \\ \mathbf{F}_m \cdot \mathbf{F}_e^* & \mathbf{F}_m \cdot \mathbf{F}_m^* \end{pmatrix} = \begin{pmatrix} W_e & W_{\text{em}} \\ W_{\text{me}} & W_m \end{pmatrix} && \text{(EM basis)} \end{aligned} \quad (35)$$

whose \mathbb{C}^2 determinant is always positive from the Cauchy-Schwarz inequality $|\mathbf{F}_e|^2 \cdot |\mathbf{F}_m|^2 \geq |\mathbf{F}_e^* \cdot \mathbf{F}_m|^2$. This tensor can be expanded into Pauli matrices following eq. (28), such that it is expressed in the different bases as:

$$\begin{aligned} \mathbf{W}_{[\text{RL}]} &= \begin{pmatrix} W_R & W_{\text{RL}} \\ W_{\text{LR}} & W_L \end{pmatrix} = \frac{W_0}{2} \begin{pmatrix} 1 & 0 \\ 0 & 1 \end{pmatrix} + \frac{W_1}{2} \underbrace{\begin{pmatrix} 0 & 1 \\ 1 & 0 \end{pmatrix}}_{\sigma_1} + \frac{W_2}{2} \underbrace{\begin{pmatrix} 0 & -i \\ i & 0 \end{pmatrix}}_{\sigma_2} + \frac{W_3}{2} \underbrace{\begin{pmatrix} 1 & 0 \\ 0 & -1 \end{pmatrix}}_{\sigma_3}, \\ \mathbf{W}_{[\text{EM}]} &= \begin{pmatrix} W_e & W_{\text{em}} \\ W_{\text{me}} & W_m \end{pmatrix} = \frac{W_0}{2} \begin{pmatrix} 1 & 0 \\ 0 & 1 \end{pmatrix} + \frac{W_1}{2} \underbrace{\begin{pmatrix} 1 & 0 \\ 0 & -1 \end{pmatrix}}_{\sigma_3} - \frac{W_2}{2} \underbrace{\begin{pmatrix} 0 & 1 \\ 1 & 0 \end{pmatrix}}_{\sigma_1} - \frac{W_3}{2} \underbrace{\begin{pmatrix} 0 & -i \\ i & 0 \end{pmatrix}}_{\sigma_2}, \\ \mathbf{W}_{[\text{PA}]} &= \begin{pmatrix} W_p & W_{\text{pa}} \\ W_{\text{ap}} & W_a \end{pmatrix} = \frac{W_0}{2} \begin{pmatrix} 1 & 0 \\ 0 & 1 \end{pmatrix} + \frac{W_1}{2} \underbrace{\begin{pmatrix} 0 & 1 \\ 1 & 0 \end{pmatrix}}_{\sigma_1} - \frac{W_2}{2} \underbrace{\begin{pmatrix} 1 & 0 \\ 0 & -1 \end{pmatrix}}_{\sigma_3} + \frac{W_3}{2} \underbrace{\begin{pmatrix} 0 & -i \\ i & 0 \end{pmatrix}}_{\sigma_2}, \end{aligned} \quad (36)$$

or, written in a basis-independent way:

$$\mathbf{W} = \frac{1}{2}(W_0\mathbf{W}_0 + W_1\mathbf{W}_1 + W_2\mathbf{W}_2 + W_3\mathbf{W}_3). \quad (37)$$

with the simple definitions:

$$\begin{aligned} W_0 &= W_e + W_m = W_p + W_a = W_R + W_L = W, \\ W_1 &= W_e - W_m, \\ W_2 &= W_a - W_p, \\ W_3 &= W_R - W_L. \end{aligned} \quad (38)$$

As proven earlier, the determinant of this tensor is always positive and independent of the basis, hence $\det(\mathbf{W}) = (W_0^2 - W_1^2 - W_2^2 - W_3^2)/4 \geq 0$. This proves that (W_1, W_2, W_3) is a vector in W -space always contained in a Bloch sphere of radius W_0 , giving rise to the *energy symmetry sphere*: a main result of our work.

Also note that one can obtain the energy-like expressions W_A using the \mathbf{W}_A operators, in a basis-independent notation (note $\mathbf{W}_A^\dagger = \mathbf{W}_A$ is Hermitian hence the following are real numbers) as:

$$W_A = \boldsymbol{\psi}^\dagger \mathbf{W}_A \boldsymbol{\psi} \in \mathbb{R}. \quad (39)$$

Other quadratic quantities

There is one big difference between Jones vectors and bispinors: the \mathbb{C}^2 components of bispinors are themselves \mathbb{C}^3 -valued vectors. The way we dealt with this in the previous section was by taking a dot product

$$\mathbf{W}_{[\text{EM}]} = (\boldsymbol{\psi} \cdot \boldsymbol{\psi}^\dagger)_{[\text{EM}]} = \begin{pmatrix} \mathbf{F}_e \cdot \mathbf{F}_e^* & \mathbf{F}_e \cdot \mathbf{F}_m^* \\ \mathbf{F}_m \cdot \mathbf{F}_e^* & \mathbf{F}_m \cdot \mathbf{F}_m^* \end{pmatrix} = \frac{1}{2} \begin{pmatrix} W_0 + W_1 & -W_2 + iW_3 \\ -W_2 - iW_3 & W_0 - W_1 \end{pmatrix}. \quad (40)$$

However one might argue that this is just one of many possible products for \mathbb{C}^3 vectors. Indeed it is the case that, for example, taking the vector cross-product leads to spin-like quantities

$$(\boldsymbol{\psi} \times \boldsymbol{\psi}^\dagger)_{[\text{EM}]} = \begin{pmatrix} \mathbf{F}_e \times \mathbf{F}_e^* & \mathbf{F}_e \times \mathbf{F}_m^* \\ \mathbf{F}_m \times \mathbf{F}_e^* & \mathbf{F}_m \times \mathbf{F}_m^* \end{pmatrix} = \frac{\omega}{2i} \begin{pmatrix} \mathbf{S}_0 + \mathbf{S}_1 & -\mathbf{S}_2 + i\mathbf{S}_3 \\ -\mathbf{S}_2 - i\mathbf{S}_3 & \mathbf{S}_0 - \mathbf{S}_1 \end{pmatrix}. \quad (41)$$

Sadly these spin-like quantities are \mathbb{R}^3 vectors, therefore, there is no canonical way to define the determinant and hence prove the existence of a spin-sphere in this way. The next product that one can take is the symmetric tensor product which leads to stress-tensor-like quantities

$$(\boldsymbol{\psi} \odot \boldsymbol{\psi}^\dagger)_{[\text{EM}]} = \begin{pmatrix} \mathbf{F}_e \odot \mathbf{F}_e^* & \mathbf{F}_e \odot \mathbf{F}_m^* \\ \mathbf{F}_m \odot \mathbf{F}_e^* & \mathbf{F}_m \odot \mathbf{F}_m^* \end{pmatrix} = \frac{1}{2} \begin{pmatrix} \mathbf{T}_0 + \mathbf{T}_1 & -\mathbf{T}_2 + i\mathbf{T}_3 \\ -\mathbf{T}_2 - i\mathbf{T}_3 & \mathbf{T}_0 - \mathbf{T}_1 \end{pmatrix} + W I_3, \quad (42)$$

where $\mathbf{I}_3 = \text{diag}(1, 1, 1)$ is the identity in \mathbb{C}^3 space. One might wonder why we used the symmetric tensor product rather than the regular one. The reason for that is that the tensor product of any two \mathbb{C}^3 vectors can be split into the symmetric and antisymmetric parts

$$\mathbf{F}_i \otimes \mathbf{F}_i^* = \frac{1}{2} \mathbf{F}_i \odot \mathbf{F}_i^* + \frac{1}{2} \mathbf{F}_i \wedge \mathbf{F}_i^* \quad (43)$$

where we use symmetric and antisymmetric outer products which are defined as $\mathbf{F} \odot \mathbf{F}^* = \mathbf{F} \otimes \mathbf{F}^* + \mathbf{F}^* \otimes \mathbf{F}$, and $\mathbf{F} \wedge \mathbf{F}^* = \mathbf{F} \otimes \mathbf{F}^* - \mathbf{F}^* \otimes \mathbf{F}$ respectively. The key observation is that a bivector $\mathbf{F}_i \wedge \mathbf{F}_i^*$ (directed plane segment with a sense of rotation) is isomorphic to a vector (directed line segments with a sense of translation) $\mathbf{F}_i \times \mathbf{F}_i^*$, this isomorphism is called Hodge duality and it is denoted as $\star(\mathbf{F}_i \times \mathbf{F}_i^*) = \mathbf{F}_i \wedge \mathbf{F}_i^*$ (see, e.g. [1, p. 38]). Another useful fact is that $\text{tr}(\mathbf{F}_i \odot \mathbf{F}_i^*) = |\mathbf{F}_i|^2$ so, together, we can write

$$\mathbf{F}_i \otimes \mathbf{F}_i^* = \frac{1}{2} [\mathbf{I}_3 |\mathbf{F}_i|^2 + (\mathbf{F}_i \odot \mathbf{F}_i^* - |\mathbf{F}_i|^2) + \star(\mathbf{F}_i \times \mathbf{F}_i^*)]$$

but this is exactly the stress tensor, spin and energy densities of field \mathbf{F}_i arranged in a single complex tensor

$$\mathbf{F}_i^* \otimes \mathbf{F}_i = \frac{1}{2} (W_i \mathbf{I}_3 + \mathbf{T}_i - i\omega \star \mathbf{S}_i) \quad (44)$$

which means that the tensor product of the bispinors contains W_A , \mathbf{T}_A and \mathbf{S}_A and no new quantities

$$(\boldsymbol{\psi} \otimes \boldsymbol{\psi}^\dagger)_{[\text{EM}]} = \frac{1}{2} \begin{pmatrix} W_0 + W_1 & -W_2 + iW_3 \\ -W_2 - iW_3 & W_0 - W_1 \end{pmatrix} \mathbf{I}_3 + \frac{1}{2} \begin{pmatrix} \mathbf{T}_0 + \mathbf{T}_1 & -\mathbf{T}_2 + i\mathbf{T}_3 \\ -\mathbf{T}_2 - i\mathbf{T}_3 & \mathbf{T}_0 - \mathbf{T}_1 \end{pmatrix} + \frac{\omega \star}{2i} \begin{pmatrix} \mathbf{S}_0 + \mathbf{S}_1 & -\mathbf{S}_2 + i\mathbf{S}_3 \\ -\mathbf{S}_2 - i\mathbf{S}_3 & \mathbf{S}_0 - \mathbf{S}_1 \end{pmatrix}. \quad (45)$$

The last observable that we introduced in the main text is the canonical linear momentum density, however, simply using $\cdot(\nabla)$ leads to a tensor that has both hermitian and non-hermitian parts in the \mathbb{C}^2 space

$$[\boldsymbol{\psi} \cdot (\nabla) \boldsymbol{\psi}^\dagger]_{[\text{EM}]} = \begin{pmatrix} \mathbf{F}_e \cdot (\nabla) \mathbf{F}_e^* & \mathbf{F}_e \cdot (\nabla) \mathbf{F}_m^* \\ \mathbf{F}_m \cdot (\nabla) \mathbf{F}_e^* & \mathbf{F}_m \cdot (\nabla) \mathbf{F}_m^* \end{pmatrix} = \frac{1}{4} \nabla \begin{pmatrix} W_0 + W_1 & -W_2 + iW_3 \\ -W_2 - iW_3 & W_0 - W_1 \end{pmatrix} + \frac{i\omega}{2} \begin{pmatrix} \mathbf{p}_0 + \mathbf{p}_1 & \mathbf{p}_2 - i\mathbf{p}_3 \\ \mathbf{p}_2 + i\mathbf{p}_3 & \mathbf{p}_0 - \mathbf{p}_1 \end{pmatrix}, \quad (46)$$

the anti-hermitian part leads to the definition of the momentum-like quantities \mathbf{p}_A , while the hermitian part only contains gradients of already defined quantities W_A .

	Quantity	EM basis	PA basis	RL basis	Description
W_0	W	$\mathbf{F}_e^* \cdot \mathbf{F}_e + \mathbf{F}_m^* \cdot \mathbf{F}_m$	$\mathbf{F}_a^* \cdot \mathbf{F}_a + \mathbf{F}_p^* \cdot \mathbf{F}_p$	$\mathbf{F}_R^* \cdot \mathbf{F}_R + \mathbf{F}_L^* \cdot \mathbf{F}_L$	total energy density
W_1	$W_e - W_m$	$\mathbf{F}_e^* \cdot \mathbf{F}_e - \mathbf{F}_m^* \cdot \mathbf{F}_m$	$2\Re(\mathbf{F}_p^* \cdot \mathbf{F}_a)$	$2\Re(\mathbf{F}_R^* \cdot \mathbf{F}_L)$	EM energy difference ^a
W_2	$W_a - W_p$	$-2\Re(\mathbf{F}_e^* \cdot \mathbf{F}_m)$	$\mathbf{F}_a^* \cdot \mathbf{F}_a - \mathbf{F}_p^* \cdot \mathbf{F}_p$	$2\Im(\mathbf{F}_R^* \cdot \mathbf{F}_L)$	$-\omega \cdot$ (reactive heli. den.) ^b
W_3	$W_R - W_L$	$-2\Im(\mathbf{F}_e^* \cdot \mathbf{F}_m)$	$2\Im(\mathbf{F}_p^* \cdot \mathbf{F}_a)$	$\mathbf{F}_R^* \cdot \mathbf{F}_R - \mathbf{F}_L^* \cdot \mathbf{F}_L$	$\omega \cdot$ (helicity density)
$\omega \mathbf{p}_0$	$\omega \mathbf{p}$	$\Im[\mathbf{F}_e^* \cdot (\nabla) \mathbf{F}_e + \mathbf{F}_m^* \cdot (\nabla) \mathbf{F}_m]$	$\Im[\mathbf{F}_a^* \cdot (\nabla) \mathbf{F}_a + \mathbf{F}_p^* \cdot (\nabla) \mathbf{F}_p]$	$\Im[\mathbf{F}_R^* \cdot (\nabla) \mathbf{F}_R + \mathbf{F}_L^* \cdot (\nabla) \mathbf{F}_L]$	canonical momentum den.
$\omega \mathbf{p}_1$	$\omega(\mathbf{p}_e - \mathbf{p}_m)$	$\Im[\mathbf{F}_e^* \cdot (\nabla) \mathbf{F}_e - \mathbf{F}_m^* \cdot (\nabla) \mathbf{F}_m]$	$\Im[\mathbf{F}_a^* \cdot (\nabla) \mathbf{F}_p - \mathbf{F}_p \cdot (\nabla) \mathbf{F}_a^*]$	$\Im[\mathbf{F}_L^* \cdot (\nabla) \mathbf{F}_R - \mathbf{F}_R \cdot (\nabla) \mathbf{F}_L^*]$	EM mom. difference
$\omega \mathbf{p}_2$	$\omega(\mathbf{p}_a - \mathbf{p}_p)$	$\Im[\mathbf{F}_e \cdot (\nabla) \mathbf{F}_m^* - \mathbf{F}_m \cdot (\nabla) \mathbf{F}_e^*]$	$\Im[\mathbf{F}_a^* \cdot (\nabla) \mathbf{F}_a - \mathbf{F}_p \cdot (\nabla) \mathbf{F}_p^*]$	$\Re[\mathbf{F}_L^* \cdot (\nabla) \mathbf{F}_R - \mathbf{F}_R \cdot (\nabla) \mathbf{F}_L^*]$	
$\omega \mathbf{p}_3$	$\omega(\mathbf{p}_R - \mathbf{p}_L)$	$\Re[\mathbf{F}_e \cdot (\nabla) \mathbf{F}_m^* - \mathbf{F}_m \cdot (\nabla) \mathbf{F}_e^*]$	$\Re[\mathbf{F}_a^* \cdot (\nabla) \mathbf{F}_p - \mathbf{F}_p \cdot (\nabla) \mathbf{F}_a^*]$	$\Im[\mathbf{F}_R^* \cdot (\nabla) \mathbf{F}_R - \mathbf{F}_L^* \cdot (\nabla) \mathbf{F}_L]$	chiral momentum den. ^c
$\omega \mathbf{S}_0$	$\omega \mathbf{S}$	$\Im[\mathbf{F}_e^* \times \mathbf{F}_e + \mathbf{F}_m^* \times \mathbf{F}_m]$	$\Im[\mathbf{F}_a^* \times \mathbf{F}_a + \mathbf{F}_p^* \times \mathbf{F}_p]$	$\Im[\mathbf{F}_R^* \times \mathbf{F}_R + \mathbf{F}_L^* \times \mathbf{F}_L]$	spin angular mom. den.
$\omega \mathbf{S}_1$	$\omega(\mathbf{S}_e - \mathbf{S}_m)$	$\Im[\mathbf{F}_e^* \times \mathbf{F}_e - \mathbf{F}_m^* \times \mathbf{F}_m]$	$2\Im(\mathbf{F}_p^* \times \mathbf{F}_a)$	$2\Im(\mathbf{F}_R^* \times \mathbf{F}_L)$	EM spin difference
$\omega \mathbf{S}_2$	$\omega(\mathbf{S}_a - \mathbf{S}_p)$	$2\Im(\mathbf{F}_e \times \mathbf{F}_m^*)$	$\Im[\mathbf{F}_a^* \times \mathbf{F}_a - \mathbf{F}_p \times \mathbf{F}_p^*]$	$-2\Re(\mathbf{F}_R^* \times \mathbf{F}_L)$	$c \cdot \Im$ (Poynting vector) ^d
$\omega \mathbf{S}_3$	$\omega(\mathbf{S}_R - \mathbf{S}_L)$	$2\Re(\mathbf{F}_e \times \mathbf{F}_m^*)$	$-2\Re(\mathbf{F}_p^* \times \mathbf{F}_a)$	$\Im[\mathbf{F}_R^* \times \mathbf{F}_R - \mathbf{F}_L^* \times \mathbf{F}_L]$	$c \cdot \Re$ (Poynting vector) ^e
\mathbf{T}_0	\mathbf{T}	$\mathbf{F}_e^* \odot \mathbf{F}_e + \mathbf{F}_m^* \odot \mathbf{F}_m - W_0 \mathbf{I}$	$\mathbf{F}_a^* \odot \mathbf{F}_a + \mathbf{F}_p^* \odot \mathbf{F}_p - W_0 \mathbf{I}$	$\mathbf{F}_R^* \odot \mathbf{F}_R + \mathbf{F}_L^* \odot \mathbf{F}_L - W_0 \mathbf{I}$	Maxwell stress tensor ^f
\mathbf{T}_1	$\mathbf{T}_e - \mathbf{T}_m$	$\mathbf{F}_e^* \odot \mathbf{F}_e - \mathbf{F}_m^* \odot \mathbf{F}_m - W_1 \mathbf{I}$	$2\Re(\mathbf{F}_p^* \odot \mathbf{F}_a) - W_1 \mathbf{I}$	$2\Re(\mathbf{F}_R^* \odot \mathbf{F}_L) - W_1 \mathbf{I}$	EM stress difference
\mathbf{T}_2	$\mathbf{T}_a - \mathbf{T}_p$	$-2\Re(\mathbf{F}_e^* \odot \mathbf{F}_m) - W_2 \mathbf{I}$	$\mathbf{F}_a^* \odot \mathbf{F}_a - \mathbf{F}_p^* \odot \mathbf{F}_p - W_2 \mathbf{I}$	$2\Im(\mathbf{F}_R^* \odot \mathbf{F}_L) - W_2 \mathbf{I}$	
\mathbf{T}_3	$\mathbf{T}_R - \mathbf{T}_L$	$-2\Im(\mathbf{F}_e^* \odot \mathbf{F}_m) - W_3 \mathbf{I}$	$2\Im(\mathbf{F}_p^* \odot \mathbf{F}_a) - W_3 \mathbf{I}$	$\mathbf{F}_R^* \odot \mathbf{F}_R - \mathbf{F}_L^* \odot \mathbf{F}_L - W_3 \mathbf{I}$	chiral stress tensor ^g

^a Reactive energy density, also called reactive power density $p_{\text{react}} = -2\omega W_1$ [2, 3] and time-averaged Lagrangian [4].

^b It is sometimes called magnetoelectric energy density [5]. Related to reactive helicity $\mathfrak{S}_{\text{react}} = -W_2/\omega$, quantity explored in [6, 7].

^c Related to canonical spin $\mathbf{s}_{\text{can}} = \mathbf{p}_3/k$ [8] and discussed in e.g. [5].

^d Imaginary part of complex Poynting vector representing flow of reactive power [3, 7].

^e Real part of complex Poynting vector representing flow of active power [3, 7].

^f Represents flux of canonical momentum density \mathbf{p}_0 .

^g Represents flux of chiral momentum density \mathbf{p}_3 .

TABLE III. Quadratic quantities in different bases, revealing the similarity with Stokes vectors.

States on the surface of the energy-symmetry sphere

The main text Fig. 2 shows six special points on the surface of the symmetry sphere given by $\mathbf{F}_i = 0$ for $i = \{e, m, p, a, R, L\}$. However, in principle, there is nothing special about those specific directions and the specific axes W_1, W_2, W_3 defined in the main text.

In the well-known \mathbb{C}^2 space of field polarisations, we typically write the electric field either in the horizontal-vertical basis, (E_h, E_v) , the diagonal-antidiagonal basis, (E_d, E_a) , or the circular basis, (E_R, E_L) , which gives rise to the three axes of the Poincare sphere $\mathcal{S}_1 = |E_h|^2 - |E_v|^2$, $\mathcal{S}_2 = |E_d|^2 - |E_a|^2$ and $\mathcal{S}_3 = |E_R|^2 - |E_L|^2$, but these are not the only three possible bases. In fact, any two orthogonal polarisations can serve as a valid basis (with coefficients E_α and E_β each being a linear combination of E_h and E_v) and correspond to an arbitrary axis $|E_\alpha|^2 - |E_\beta|^2$ on the Poincare sphere with some specific orientation. Similarly, our isomorphic \mathbb{C}^2 space of bispinors admits infinitely many basis choices, apart from the EM, PA, RL basis, each with vector-valued coefficients \mathbf{F}_α and \mathbf{F}_β that are each some linear combination of $\sqrt{\varepsilon}\mathbf{E}$ and $\sqrt{\mu}\mathbf{H}$. In that basis one can write $\psi_{[\alpha\beta]} = (\mathbf{F}_\alpha, \mathbf{F}_\beta)$. This basis will represent an axis going through the origin of the symmetry sphere, with the axis value associated to the quantity $|\mathbf{F}_\alpha|^2 - |\mathbf{F}_\beta|^2$. Reversing the argument, every axis crossing the origin of the symmetry sphere, regardless of orientation, will have some associated basis whose vector coefficients are $(\mathbf{F}_{i\alpha}, \mathbf{F}_{i\beta})$.

This means that every point lying exactly on the surface of the symmetry sphere (where $W_1^2 + W_2^2 + W_3^2 = W_0^2$) corresponds to a point where a given $\mathbf{F}_{i\alpha} = 0$. Because $\mathbf{F}_{i\alpha}$ is always a linear combination of $\sqrt{\varepsilon}\mathbf{E}$ and $\sqrt{\mu}\mathbf{H}$, the surface of the field-symmetry sphere necessarily corresponds to electromagnetic states where both quantities are linearly dependent, such that their linear combination can be zero. Hence, on the surface of the symmetry sphere, $\sqrt{\varepsilon}\mathbf{E} = \delta\sqrt{\mu}\mathbf{H}$ with δ a complex scalar. With some algebra, one can find that for any arbitrary location on the surface of the field-symmetry sphere, with spherical angle coordinates (θ_i, ϕ_i) measured with respect to the arbitrary axis corresponding to $|\mathbf{F}_{i\alpha}|^2 - |\mathbf{F}_{i\beta}|^2$ acting as polar axis, the linear dependence of the fields is given specifically by:

$$\sin(\theta_i/2)\mathbf{F}_{i\alpha} = e^{i\phi_i} \cos(\theta_i/2)\mathbf{F}_{i\beta}, \quad (47)$$

such that the polar angle θ_i determines the amplitude ratio, while the azimuthal angle ϕ_i determines the relative phase between the basis coefficients $\mathbf{F}_{i\alpha}$ and $\mathbf{F}_{i\beta}$. This relation is a well-known property of a Bloch sphere, often used in quantum superpositions of two states.

If we choose to express this in terms of \mathbf{E} and \mathbf{H} , this is equivalent to choosing the EM basis $\psi = (\mathbf{F}_e, \mathbf{F}_m)$ to describe the fields and define the angles on the sphere (θ_1, ϕ_1) , such that the W_1 axis plays the role of polar axis. In this case, eq. (47) can be written as:

$$\sin(\theta_1/2)\sqrt{\varepsilon}\mathbf{E} = e^{i\phi_1} \cos(\theta_1/2)\sqrt{\mu}\mathbf{H}, \quad (48)$$

or, equivalently:

$$\mathbf{E} = \underbrace{\frac{e^{i\phi_1}}{\tan(\theta_1/2)}}_{\delta(\theta_1, \phi_1)} \eta \mathbf{H}, \quad (49)$$

which provides the linear relationship between the \mathbf{E} and \mathbf{H} field corresponding to any point in the surface of the energy symmetry sphere. Six such special points (corresponding to the antipodes for the bases EM, PA, RL, where the sphere intersects the W_1, W_2 and W_3 axes) are shown in Fig. 2 of the main text.

Electromagnetic symmetry sphere for dipolar fields

Entire three-dimensional electromagnetic fields including near and far field regions can be mapped into the volume of the electromagnetic symmetry sphere, constructing complicated 3D patterns that measure the share of energy density among $W_{1,2,3}$. In this section we map well-known dipolar fields to the symmetry sphere as well as ‘synthetic’ dipoles inspired by the vectors \mathbf{F}_A in the main article. Each example is a superposition of an electric dipole with dipole moment $\mathbf{p} = (p_x, p_y, p_z)$ and a magnetic dipole with dipole moment $\mathbf{m} = (m_x, m_y, m_z)$ —this way, an x -polarised electric dipole is given by $(p_x, p_y, p_z) = (1, 0, 0)$ and $(m_x, m_y, m_z) = \mathbf{0}$ both superimposed at the origin. The full electromagnetic fields in free space created by such a magnetoelectric dipole are well known [3] and given in SI units by:

$$\mathbf{E}(\mathbf{r}) = \frac{1}{4\pi\epsilon_0} \left\{ k^2(\hat{\mathbf{r}} \times \mathbf{p}) \times \hat{\mathbf{r}} \frac{e^{ikr}}{r} + [3(\hat{\mathbf{r}} \cdot \mathbf{p})\hat{\mathbf{r}} - \mathbf{p}] \left(\frac{1}{r^3} - \frac{ik}{r^2} \right) e^{ikr} \right\} - \frac{\eta k^2}{4\pi} (\hat{\mathbf{r}} \times \mathbf{m}) \left(1 - \frac{1}{ikr} \right) \frac{e^{ikr}}{r} \quad (50)$$

$$\mathbf{H}(\mathbf{r}) = \frac{ck^2}{4\pi} (\hat{\mathbf{r}} \times \mathbf{p}) \left(1 - \frac{1}{ikr} \right) \frac{e^{ikr}}{r} + \frac{1}{4\pi} \left\{ k^2(\hat{\mathbf{r}} \times \mathbf{m}) \times \hat{\mathbf{r}} \frac{e^{ikr}}{r} + [3(\hat{\mathbf{r}} \cdot \mathbf{m})\hat{\mathbf{r}} - \mathbf{m}] \left(\frac{1}{r^3} - \frac{ik}{r^2} \right) e^{ikr} \right\} \quad (51)$$

where ϵ_0 is the permittivity of free space, $k = \omega/c = 2\pi/\lambda$ is the wavenumber of free space, $\eta = \sqrt{\mu_0/\epsilon_0}$ is the impedance of free space, $\hat{\mathbf{r}} = \mathbf{r}/r$ is the unit vector in the radial direction, and \mathbf{r} is the position vector, with length r .

In Fig. S1, the symmetry sphere mapping is calculated for a selection of dipoles. To complete the mapping the real-space fields of each dipole (given by eqs. (50) and (51)) are calculated in a spherical volume of radius equal to the wavelength λ and sampled uniformly in a spatial grid—for each sample the energy densities $W_{1,2,3}$ are calculated and normalised by the local total energy density W_0 to place a marker in the symmetry sphere. Markers are colour coded to represent the radial distance of the real-space field sample from the dipole; red markers are furthest from the dipolar source, approaching the far field, while blue coloured markers correspond to near fields. With this approach, the symmetry sphere for the fields surrounding different electric-magnetic dipoles are shown in fig. S1.

Circular electric and magnetic dipoles (a) and (b) build helical structures (with the same winding sense) within the symmetry sphere while the entire electromagnetic field of the Janus dipole [9] (c) maps to the W_2W_3 plane. The mapped structures in (a) and (b) can be interchanged visually by a \hat{D} transformation which rotates the sphere 180 degrees about the W_3 axis. As anticipated in these cases, paraxial far fields collapse on to the W_3 axis, indicated by the aggregation of the red markers. Perhaps confusingly the Huygens dipole field (d), while sitting in the W_1W_2 plane, does not completely collapse onto the W_3 axis in the far field as shown by the red markers interspersed with near field samples, some situated virtually at the sphere equator. This occurs because, unlike the other three dipole fields, the Huygens dipole has a dark spot in its far field radiation pattern where transverse field components vanish. Approaching this dark spot, radial and transverse field components inevitably become comparable resulting in a small far-field non-paraxial region [10] where it is possible for $W_{1,2}$ to be large relative to the (albeit strongly suppressed) total energy density W_0 (note once more that the sphere axes are normalised by W_0). In (e), a circularly polarised Janus dipole produces a rotated version of the ordinary Janus dipole’s symmetry sphere structure, while in (f)-(h) are more ‘elementary’ dipoles which only have one component in the \mathbb{C}^2 space of the dipole moment bispinor. These elementary dipoles are (f): a π_e dipole (an electric dipole), (g): a π_p dipole and (h): a π_R dipole—each of these dipoles has given \mathbf{p} and \mathbf{m} dipole moments which eliminate the π_m , π_a and π_L components in Eq. 57 from (f)-(h) respectively. The electric dipole (f) radiates a field whose energy density is largely supplied by the electric field more than the magnetic field, hence in the symmetry sphere its field maps onto the positive W_1 axis (with a small tail on the negative side of that axis). Meanwhile a similar situation occurs in (g) as the π_p dipole field maps mostly to the negative W_2 axis. In (h) is shown the striking feature of a π_R dipole which is that its entire radiated field is right-handed, mapping to a single point at the north pole of the symmetry sphere.

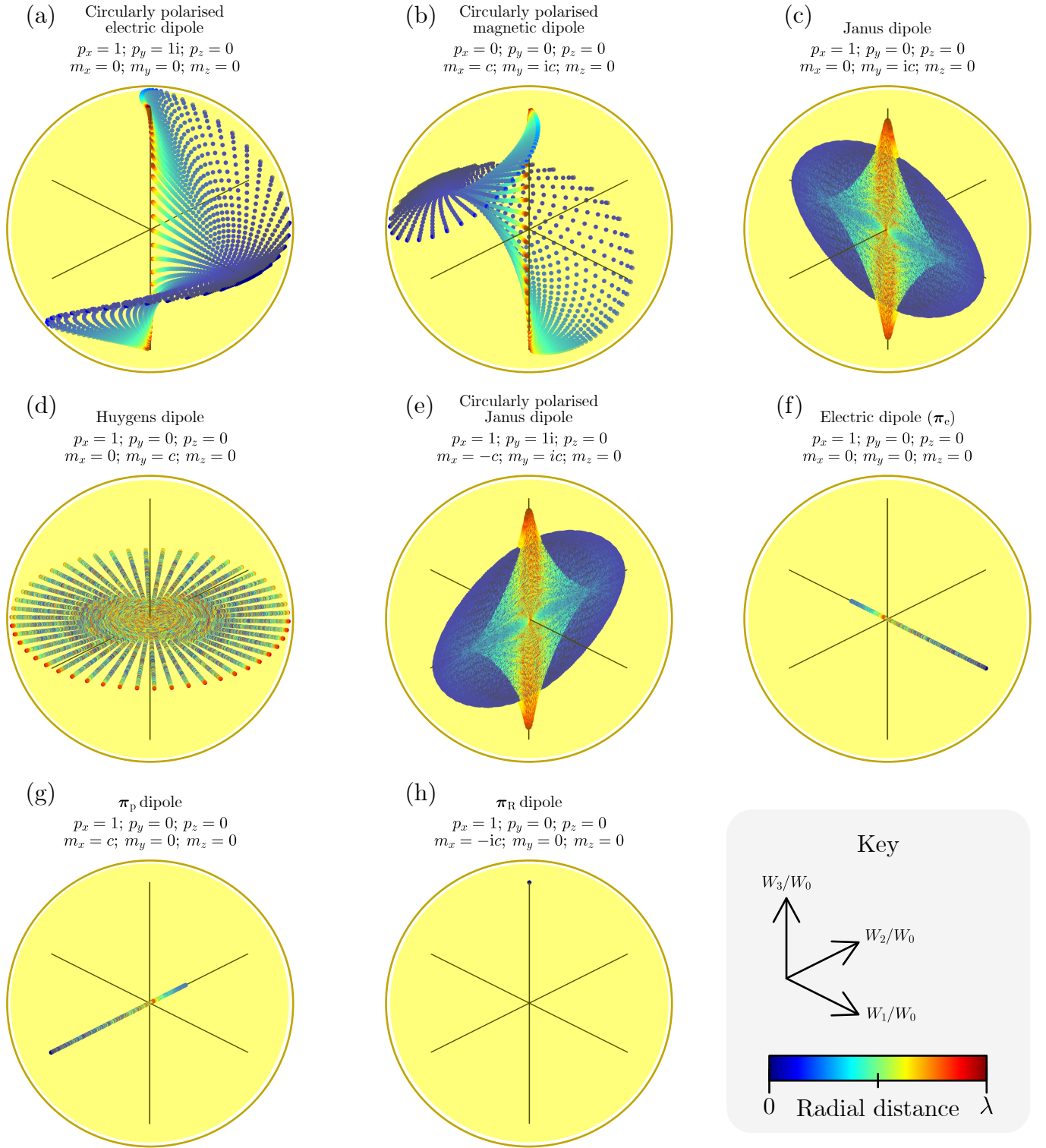


FIG. S1. The electromagnetic fields produced in a 1λ -radius volume by an assortment of dipoles, mapped to the symmetry sphere with axes normalised by total energy density W_0 . Each marker in the sphere corresponds to a sample of the dipole field in real space. The colour of the marker corresponds to its radial distance from the dipole up to λ (red markers are real-space samples approaching the far field).

Maxwell-like equations with field quadratic quantities

The dual-symmetric (including magnetic charges) time-harmonic Maxwell's equations in eq. (17), written in a more standard notation, are:

$$\begin{aligned}
\nabla \cdot \mathbf{E} &= \rho_e / \varepsilon, \\
\nabla \cdot \mathbf{H} &= \rho_m / \mu, \\
\nabla \times \mathbf{E} &= +ik\eta \mathbf{H} - \mathbf{J}_m, \\
\nabla \times \mathbf{H} &= -ik\mathbf{E} / \eta + \mathbf{J}_e.
\end{aligned} \tag{52}$$

In the main text we mention that certain combination of the spin-like quadratic quantities $(\mathbf{S}_0, \mathbf{S}_1, \mathbf{S}_2, \mathbf{S}_3)$ fulfil Maxwell-like equations. Indeed, from eq. (6) in the main text, one can check that the complex combinations $\mathbf{S}_0 \pm i\mathbf{S}_3$ satisfy the following equations:

$$\begin{aligned}
\nabla \cdot (\mathbf{S}_0 \pm i\mathbf{S}_3) &= 0, \\
\nabla \times (\mathbf{S}_0 \pm i\mathbf{S}_3) &= \pm 2ik(\mathbf{S}_0 \mp i\mathbf{S}_3) - 2(\mathbf{p}_0 \pm i\mathbf{p}_3),
\end{aligned} \tag{53}$$

making them exactly analogous to time harmonic electric and magnetic fields with twice the frequency of the fields and with currents but no charge densities. Also, the equivalent of duality symmetry of these quantities is simply complex conjugation or parity. One can combine these into a single Helmholtz equation

$$(\nabla^2 + 4k^2)(\mathbf{S}_0 \pm i\mathbf{S}_3) = 4k(\mathbf{p}_3 \pm i\mathbf{p}_0) + 2\nabla \times (\mathbf{p}_0 \pm i\mathbf{p}_3). \tag{54}$$

The remaining two spin-like quadratic quantities can also be combined into a complex quantity, however, this time they will be quasistatic fields (taking $k = 0$ in eq. (52) and resembling electrostatic/magnetostatic fields) with both charge densities currents

$$\begin{aligned}
\nabla \cdot (\mathbf{S}_1 \pm i\mathbf{S}_2) &= \frac{2}{c}(W_2 \mp iW_1), \\
\nabla \times (\mathbf{S}_1 \pm i\mathbf{S}_2) &= -2(\mathbf{p}_1 \mp i\mathbf{p}_2),
\end{aligned} \tag{55}$$

These can be combined into a single Poisson equation

$$(\nabla^2 + 0k^2)(\mathbf{S}_1 \pm i\mathbf{S}_2) = \frac{2}{c}\nabla(W_2 \mp iW_1) + 2\nabla \times (\mathbf{p}_1 \mp i\mathbf{p}_2). \tag{56}$$

In the same way in which $\mathbf{S}_0 \pm i\mathbf{S}_3$ fulfils the Helmholtz equation with twice the frequency of the fields $\mathbf{S}_1 \pm i\mathbf{S}_2$ fulfils the Poisson equation (Helmholtz equation with zero times the frequency).

LIGHT-MATTER INTERACTION ON DIFFERENT \mathbb{C}^2 BASES

The dipole moment bispinor and basis-independent polarisability

In the same way that electric and magnetic fields may be combined into an electromagnetic bi-spinor ψ , so can electric \mathbf{p} and magnetic \mathbf{m} dipole moments be combined into a dipole moment bispinor π , which can be written in each of the three bases:

$$\begin{aligned}
\pi_{\text{EM}}(\mathbf{r}) &= \begin{pmatrix} \pi_e \\ \pi_m \end{pmatrix} = \frac{1}{2} \begin{pmatrix} \mathbf{p}/\sqrt{\varepsilon} \\ \sqrt{\mu}\mathbf{m} \end{pmatrix}, \\
\pi_{\text{PA}}(\mathbf{r}) &= \begin{pmatrix} \pi_p \\ \pi_a \end{pmatrix} = \frac{1}{2\sqrt{2}} \begin{pmatrix} \mathbf{p}/\sqrt{\varepsilon} + \sqrt{\mu}\mathbf{m} \\ \mathbf{p}/\sqrt{\varepsilon} - \sqrt{\mu}\mathbf{m} \end{pmatrix}, \\
\pi_{\text{RL}}(\mathbf{r}) &= \begin{pmatrix} \pi_R \\ \pi_L \end{pmatrix} = \frac{1}{2\sqrt{2}} \begin{pmatrix} \mathbf{p}/\sqrt{\varepsilon} + i\sqrt{\mu}\mathbf{m} \\ \mathbf{p}/\sqrt{\varepsilon} - i\sqrt{\mu}\mathbf{m} \end{pmatrix},
\end{aligned} \tag{57}$$

In a Rayleigh particle, the linearity of the response ensures that the dipole moments induced in the particle are proportional to the applied fields via a polarisability matrix. In a basis-independent bi-spinor notation, this is written:

$$\pi = \mathbf{A}\psi \tag{58}$$

For isotropic particles, the polarisability matrix \mathbf{A} can be represented in any basis as a two-by-two complex-valued matrix, and hence we can apply the results from eq. (28), as we do below:

$$\begin{aligned}\boldsymbol{\pi}_{\text{EM}} &= \begin{pmatrix} \boldsymbol{\pi}_{\text{e}} \\ \boldsymbol{\pi}_{\text{m}} \end{pmatrix} = \begin{pmatrix} \alpha_{\text{e}} & \alpha_{\text{em}} \\ \alpha_{\text{me}} & \alpha_{\text{m}} \end{pmatrix} \begin{pmatrix} \mathbf{F}_{\text{e}} \\ \mathbf{F}_{\text{m}} \end{pmatrix} = \left[\alpha_0 \begin{pmatrix} 1 & 0 \\ 0 & 1 \end{pmatrix} + \alpha_1 \underbrace{\begin{pmatrix} 1 & 0 \\ 0 & -1 \end{pmatrix}}_{\sigma_3} - \alpha_2 \underbrace{\begin{pmatrix} 0 & 1 \\ 1 & 0 \end{pmatrix}}_{\sigma_1} - \alpha_3 \underbrace{\begin{pmatrix} 0 & -i \\ i & 0 \end{pmatrix}}_{\sigma_2} \right] \begin{pmatrix} \mathbf{F}_{\text{e}} \\ \mathbf{F}_{\text{m}} \end{pmatrix}, \\ \boldsymbol{\pi}_{\text{PA}} &= \begin{pmatrix} \boldsymbol{\pi}_{\text{p}} \\ \boldsymbol{\pi}_{\text{a}} \end{pmatrix} = \begin{pmatrix} \alpha_{\text{p}} & \alpha_{\text{pa}} \\ \alpha_{\text{ap}} & \alpha_{\text{a}} \end{pmatrix} \begin{pmatrix} \mathbf{F}_{\text{p}} \\ \mathbf{F}_{\text{a}} \end{pmatrix} = \left[\alpha_0 \begin{pmatrix} 1 & 0 \\ 0 & 1 \end{pmatrix} + \alpha_1 \underbrace{\begin{pmatrix} 0 & 1 \\ 1 & 0 \end{pmatrix}}_{\sigma_1} - \alpha_2 \underbrace{\begin{pmatrix} 1 & 0 \\ 0 & -1 \end{pmatrix}}_{\sigma_3} + \alpha_3 \underbrace{\begin{pmatrix} 0 & -i \\ i & 0 \end{pmatrix}}_{\sigma_2} \right] \begin{pmatrix} \mathbf{F}_{\text{p}} \\ \mathbf{F}_{\text{a}} \end{pmatrix}, \\ \boldsymbol{\pi}_{\text{RL}} &= \begin{pmatrix} \boldsymbol{\pi}_{\text{R}} \\ \boldsymbol{\pi}_{\text{L}} \end{pmatrix} = \begin{pmatrix} \alpha_{\text{R}} & \alpha_{\text{RL}} \\ \alpha_{\text{LR}} & \alpha_{\text{L}} \end{pmatrix} \begin{pmatrix} \mathbf{F}_{\text{R}} \\ \mathbf{F}_{\text{L}} \end{pmatrix} = \left[\alpha_0 \begin{pmatrix} 1 & 0 \\ 0 & 1 \end{pmatrix} + \alpha_1 \underbrace{\begin{pmatrix} 0 & 1 \\ 1 & 0 \end{pmatrix}}_{\sigma_1} + \alpha_2 \underbrace{\begin{pmatrix} 0 & -i \\ i & 0 \end{pmatrix}}_{\sigma_2} + \alpha_3 \underbrace{\begin{pmatrix} 1 & 0 \\ 0 & -1 \end{pmatrix}}_{\sigma_3} \right] \begin{pmatrix} \mathbf{F}_{\text{R}} \\ \mathbf{F}_{\text{L}} \end{pmatrix},\end{aligned}\quad (59)$$

which provides us with four basis-independent measures of polarisability following eq. (29):

$$\begin{aligned}\alpha_0 &= \frac{1}{2}(\alpha_{\text{R}} + \alpha_{\text{L}}) = \frac{1}{2}(\alpha_{\text{e}} + \alpha_{\text{m}}) = \frac{1}{2}(\alpha_{\text{p}} + \alpha_{\text{a}}), \\ \alpha_1 &= \frac{1}{2}(\alpha_{\text{e}} - \alpha_{\text{m}}), \\ \alpha_2 &= -\frac{1}{2}(\alpha_{\text{p}} - \alpha_{\text{a}}), \\ \alpha_3 &= \frac{1}{2}(\alpha_{\text{R}} - \alpha_{\text{L}}).\end{aligned}\quad (60)$$

Most readers are familiar with the EM basis notation, $\boldsymbol{\pi}_{\text{EM}}$ above. Note that in that representation, the main diagonal is composed exclusively of α_0 and α_1 , providing the sum and difference of electric and magnetic polarisabilities, while the off-diagonal components in $\boldsymbol{\pi}_{\text{EM}}$ are the antisymmetric α_3 , termed the chiral polarisability, and the symmetric α_2 , the non-reciprocal polarisability. By changing the basis, we can see that the chiral polarisability α_3 is also the difference in the main diagonal elements in the RL basis. This insight is not new, but we believe that eq. (60) constitutes a very intuitive explanation. Similarly, α_2 is the difference in the main diagonal elements in the PA basis. Because the three matrices in eq. (59) are *similar matrices*, they share the same trace and determinant in \mathbb{C}^2 space:

$$\begin{aligned}\text{tr}\{\mathbf{A}\} &= \alpha_{\text{e}} + \alpha_{\text{m}} = \alpha_{\text{p}} + \alpha_{\text{a}} = \alpha_{\text{R}} + \alpha_{\text{L}} = 2\alpha_0, \\ \det\{\mathbf{A}\} &= \alpha_{\text{e}}\alpha_{\text{m}} - \alpha_{\text{em}}\alpha_{\text{me}} = \alpha_{\text{p}}\alpha_{\text{a}} - \alpha_{\text{pa}}\alpha_{\text{ap}} = \alpha_{\text{R}}\alpha_{\text{L}} - \alpha_{\text{RL}}\alpha_{\text{LR}} = \alpha_0^2 - \alpha_1^2 - \alpha_2^2 - \alpha_3^2.\end{aligned}\quad (61)$$

In general the response of a particle can be non-isotropic in the \mathbb{C}^3 space. In that case the components α_i with $i \in \{\text{e,m,p,a,R,L}\}$ will become three-by-three matrices $\boldsymbol{\alpha}_i$ (same for α_A with $A \in \{0,1,2,3\}$) and the full response \mathbf{A} can be thought of as a six-by-six matrix. Note however, that same as one can treat the \mathbb{C}^2 and \mathbb{C}^3 as separate vector spaces the same is true for the matrices acting on them. This means that eqs. (59) and (60) will be the same just with $\alpha_i \mapsto \boldsymbol{\alpha}_i$, more care has to be taken in case of eq. (61) as one also has to emphasise that $\text{tr} \mapsto \text{tr}_{\mathbb{C}^2}$ and $\det \mapsto \det_{\mathbb{C}^2}$ are taken only across the two-by-two components that act on \mathbb{C}^2 .

The use of these bases in \mathbb{C}^2 space also brings great simplifications to the analytical calculations involving dipoles. For instance, the power extinguished by a dipolar particle has the well known analytical expression:

$$P_{\text{ext}} = \frac{\omega}{2} \Im(\mathbf{E}^* \cdot \mathbf{p} + \mu \mathbf{H}^* \cdot \mathbf{m}), \quad (62)$$

this can be written in a basis-independent way as a dot product of the electromagnetic and dipolar bi-spinors [5]:

$$P_{\text{ext}} = 2\omega \Im(\boldsymbol{\psi}^\dagger \cdot \boldsymbol{\pi}), \quad (63)$$

by applying the linear relation between dipolar bispinor and electromagnetic bispinor $\boldsymbol{\pi} = \mathbf{A}\boldsymbol{\psi}$ (eq. (58)), followed by the basis-independent decomposition $\mathbf{A} = \alpha_0 \mathbf{W}_0 + \alpha_1 \mathbf{W}_1 + \alpha_2 \mathbf{W}_2 + \alpha_3 \mathbf{W}_3$ (eq. (27)), we will get

$$P_{\text{ext}} = 2\omega \Im(\boldsymbol{\psi}^\dagger \cdot \mathbf{A}\boldsymbol{\psi}) = 2\omega \Im[\boldsymbol{\psi}^\dagger \cdot (\alpha_0 \mathbf{W}_0 + \alpha_1 \mathbf{W}_1 + \alpha_2 \mathbf{W}_2 + \alpha_3 \mathbf{W}_3)\boldsymbol{\psi}],$$

if the particle is isotropic then α_A are scalar and can be pulled through $\boldsymbol{\psi}^\dagger$ to obtain

$$P_{\text{ext}} = 2\omega \sum_{A=0}^3 \Im[\alpha_A (\boldsymbol{\psi}^\dagger \mathbf{W}_A \boldsymbol{\psi})],$$

and using the relation $W_A = \psi^\dagger \mathbf{W}_A \psi$ (eq. (39)), one can derive:

$$P_{\text{ext}} = 2\omega \sum_{A=0}^3 \Im(\alpha_A) W_A.$$

This leads to a remarkably simple expression for the extinction power, revealing the deep link between the energy-symmetry sphere coordinates W_i and the polarisability-sphere parameters α_i :

$$P_{\text{ext}} = 2\omega [\Im(\alpha_0)W_0 + \Im(\alpha_1)W_1 + \Im(\alpha_2)W_2 + \Im(\alpha_3)W_3]. \quad (64)$$

One can also define generalised intensities cW_A and extinction cross sections to write $\sigma_A^{\text{ext}} = 2k\Im(\alpha_A)$

$$P_{\text{ext}} = \sigma_0^{\text{ext}} cW_0 + \sigma_1^{\text{ext}} cW_1 + \sigma_2^{\text{ext}} cW_2 + \sigma_3^{\text{ext}} cW_3. \quad (65)$$

This carries much insight. For instance, as we showed that paraxial far fields have $W_1 = W_2 = 0$, this reveals that we cannot retrieve α_1 and α_2 by using far-field dipolar extinction measurements (we cannot distinguish between electric and magnetic polarisability, or retrieve the non-reciprocal polarisability). While α_0 and α_3 are usually measured, using far-field illumination, as the extinction cross section $\sigma_{\text{ext}} = 2k\Im(\alpha_0) = k\Im(\alpha_e + \alpha_m)$ and the g -factor $g = 2\Im(\alpha_3)/\Im(\alpha_0)$ spectra, which can then be used to obtain real parts using Kramers–Kronig relations. Similar simple expressions can be derived for dipolar absorption, force and torque [5].

Macroscopic Maxwell equations

So far we have considered microscopic Maxwell equations and point particles, so we have been limited to homogeneous materials with no structure. If we want to consider material structures, such as finite particles, waveguides, etc., we need to turn to the macroscopic Maxwell equations. Consider \mathbf{J}_e and \mathbf{J}_m to be only the *free* currents

$$\begin{aligned} \nabla \times \mathbf{E} &= -\frac{\partial \mathbf{B}}{\partial t} - \mathbf{J}_m, \\ \nabla \times \mathbf{H} &= \frac{\partial \mathbf{D}}{\partial t} + \mathbf{J}_e, \end{aligned} \quad (66)$$

which in the time-harmonic case ($\partial/\partial t \rightarrow -i\omega \rightarrow -ik_0c_0$, with $k_0 = \omega/c_0$) become:

$$\begin{aligned} \nabla \times \mathbf{E} &= ik_0c_0\mathbf{B} - \mathbf{J}_m, \\ \nabla \times \mathbf{H} &= -ik_0c_0\mathbf{D} + \mathbf{J}_e. \end{aligned} \quad (67)$$

Now, substituting $c_0 = 1/\sqrt{\varepsilon_0\mu_0}$, we can write these two equations as a single equation in bi-spinor (\mathbb{C}^2) space (and this will be in the EM basis) [11]:

$$\begin{aligned} \begin{pmatrix} \nabla \times & 0 \\ 0 & \nabla \times \end{pmatrix} \frac{1}{2} \begin{pmatrix} \sqrt{\varepsilon_0} \mathbf{E} \\ \sqrt{\mu_0} \mathbf{H} \end{pmatrix} &= ik_0 \frac{1}{2} \begin{pmatrix} \mathbf{B}/\sqrt{\mu_0} \\ -\mathbf{D}/\sqrt{\varepsilon_0} \end{pmatrix} - \frac{1}{2} \begin{pmatrix} \mathbf{J}_m \\ -\mathbf{J}_e \end{pmatrix}, \\ \begin{pmatrix} \nabla \times & 0 \\ 0 & \nabla \times \end{pmatrix} \frac{1}{2} \underbrace{\begin{pmatrix} \sqrt{\varepsilon_0} \mathbf{E} \\ \sqrt{\mu_0} \mathbf{H} \end{pmatrix}}_{\psi_{\text{EM}} = \begin{pmatrix} \mathbf{F}_e \\ \mathbf{F}_m \end{pmatrix}} &= \underbrace{\begin{pmatrix} 0 & 1 \\ -1 & 0 \end{pmatrix}}_{\hat{D}_{\text{EM}}} \left[ik_0 \underbrace{\frac{1}{2} \begin{pmatrix} \mathbf{D}/\sqrt{\varepsilon_0} \\ \mathbf{B}/\sqrt{\mu_0} \end{pmatrix}}_{\gamma_{\text{EM}} = \begin{pmatrix} \mathbf{G}_e \\ \mathbf{G}_m \end{pmatrix}} - \frac{1}{2} \underbrace{\begin{pmatrix} \mathbf{J}_e \\ \mathbf{J}_m \end{pmatrix}}_{\mathbf{g}_{\text{EM}}} \right], \end{aligned} \quad (68)$$

which motivates us to introduce a bi-spinor with the auxiliary displacement-field \mathbf{D} and magnetic flux \mathbf{B} , which we define as $\boldsymbol{\gamma} = (\mathbf{D}/2\sqrt{\varepsilon_0})\hat{\mathbf{e}} + (\mathbf{B}/2\sqrt{\mu_0})\hat{\mathbf{m}} = \mathbf{G}_e\hat{\mathbf{e}} + \mathbf{G}_m\hat{\mathbf{m}}$. Note that the prefactors are the *vacuum* permittivity and permeability, and are there just to make the dimensions match. We are *not* assuming a vacuum background, as the information of the material is encoded in the constitutive relations between the fields and auxiliary fields. We also used the duality transformation \hat{D} such that $i\hat{D} = \mathbf{W}_3$, following table II, corresponds to the Pauli matrix $-\boldsymbol{\sigma}_2 = i\hat{D} = i\begin{pmatrix} 0 & 1 \\ -1 & 0 \end{pmatrix}$ in the EM basis above. The remaining two equations can be obtained from the microscopic ones eq. (24) simply by $\psi \mapsto \boldsymbol{\gamma}$ and considering \mathbf{f} to be free charges. The macroscopic Maxwell's equations can thus be written in a \mathbb{C}^2 -basis-independent form as:

$$\begin{aligned} \nabla \cdot \boldsymbol{\gamma} &= \mathbf{f}, \\ \nabla \times \boldsymbol{\psi} &= \hat{D}(ik_0\boldsymbol{\gamma} - \mathbf{g}). \end{aligned} \quad (69)$$

Constitutive relations

Now, we will focus on the case of linear and isotropic materials (but including chiral and non-reciprocal properties). The constitutive relations are well known, and we will write them in a compact notation focusing on susceptibilities, :

$$\underbrace{\frac{1}{2} \begin{pmatrix} \mathbf{D}/\sqrt{\varepsilon_0} \\ \mathbf{B}/\sqrt{\mu_0} \end{pmatrix}}_{\boldsymbol{\gamma}_{\text{EM}} = \begin{pmatrix} \mathbf{G}_e \\ \mathbf{G}_m \end{pmatrix}} = \underbrace{\begin{pmatrix} \overbrace{1 + \chi_e}^{\varepsilon_r} & \chi_t + i\chi_c \\ \chi_t - i\chi_c & \overbrace{1 + \chi_m}^{\mu_r} \end{pmatrix}}_{\mathbf{I} + \boldsymbol{\chi}_{\text{EM}}} \underbrace{\frac{1}{2} \begin{pmatrix} \sqrt{\varepsilon_0} \mathbf{E} \\ \sqrt{\mu_0} \mathbf{H} \end{pmatrix}}_{\boldsymbol{\psi}_{\text{EM}} = \begin{pmatrix} \mathbf{F}_e \\ \mathbf{F}_m \end{pmatrix}} \quad (70)$$

where χ_e is the electric susceptibility, $\varepsilon_r = 1 + \chi_e$ the relative electric permittivity, χ_m the magnetic susceptibility, $\mu_r = 1 + \chi_m$ the relative magnetic permeability, χ_c is a chiral susceptibility (typically written as the κ material parameter in many works), and χ_t the non-reciprocal susceptibility. This means that the constitutive relations can be written in a basis-independent notation of bi-spinors as:

$$\boldsymbol{\gamma} = (\mathbf{I} + \boldsymbol{\chi})\boldsymbol{\psi} \quad (71)$$

where the tensor $\boldsymbol{\chi}$ in \mathbb{C}^2 space can, following eq. (28), be written in different bases:

$$\begin{aligned} \boldsymbol{\chi}_{[\text{RL}]} &= \begin{pmatrix} \chi_R & \chi_{\text{RL}} \\ \chi_{\text{LR}} & \chi_L \end{pmatrix} = \chi_0 \begin{pmatrix} 1 & 0 \\ 0 & 1 \end{pmatrix} + \chi_1 \underbrace{\begin{pmatrix} 0 & 1 \\ 1 & 0 \end{pmatrix}}_{\sigma_1} + \chi_2 \underbrace{\begin{pmatrix} 0 & -i \\ i & 0 \end{pmatrix}}_{\sigma_2} + \chi_3 \underbrace{\begin{pmatrix} 1 & 0 \\ 0 & -1 \end{pmatrix}}_{\sigma_3}, \\ \boldsymbol{\chi}_{[\text{EM}]} &= \begin{pmatrix} \chi_e & \chi_{\text{em}} \\ \chi_{\text{me}} & \chi_m \end{pmatrix} = \chi_0 \begin{pmatrix} 1 & 0 \\ 0 & 1 \end{pmatrix} + \chi_1 \underbrace{\begin{pmatrix} 1 & 0 \\ 0 & -1 \end{pmatrix}}_{\sigma_3} - \chi_2 \underbrace{\begin{pmatrix} 0 & 1 \\ 1 & 0 \end{pmatrix}}_{\sigma_1} - \chi_3 \underbrace{\begin{pmatrix} 0 & -i \\ i & 0 \end{pmatrix}}_{\sigma_2}, \\ \boldsymbol{\chi}_{[\text{PA}]} &= \begin{pmatrix} \chi_p & \chi_{\text{pa}} \\ \chi_{\text{ap}} & \chi_a \end{pmatrix} = \chi_0 \begin{pmatrix} 1 & 0 \\ 0 & 1 \end{pmatrix} + \chi_1 \underbrace{\begin{pmatrix} 0 & 1 \\ 1 & 0 \end{pmatrix}}_{\sigma_1} - \chi_2 \underbrace{\begin{pmatrix} 1 & 0 \\ 0 & -1 \end{pmatrix}}_{\sigma_3} + \chi_3 \underbrace{\begin{pmatrix} 0 & -i \\ i & 0 \end{pmatrix}}_{\sigma_2}, \end{aligned} \quad (72)$$

which provides the definition of the following four basis-independent degrees of freedom of the susceptibility tensor:

$$\begin{aligned} \chi_0 &= \frac{1}{2}(\varepsilon_r + \mu_r) - 1 = \frac{1}{2}(\chi_e + \chi_m) = \frac{1}{2}(\chi_R + \chi_L) = \frac{1}{2}(\chi_p + \chi_a), \\ \chi_1 &= \frac{1}{2}(\varepsilon_r - \mu_r) = \frac{1}{2}(\chi_e - \chi_m), \\ \chi_2 &= -\chi_t = -\frac{1}{2}(\chi_p - \chi_a), \\ \chi_3 &= \chi_c = \frac{1}{2}(\chi_R - \chi_L). \end{aligned} \quad (73)$$

These four susceptibilities will completely define any isotropic linear medium in a basis-independent way, unlike most formulations that give special importance to the EM basis. Note that each of these susceptibilities $\chi_A(\mathbf{r})$ may be a function of position, defining any geometry, in the same way that a position-dependent $\varepsilon_r(\mathbf{r})$ is often used to describe dielectric systems such as particles, slabs, waveguides, etc.

Diagonalisation of macroscopic Maxwell equations

Combining the \mathbb{C}^2 -basis-independent formulation of the macroscopic Maxwell equation (with no *free* charges and currents) $\nabla \times \boldsymbol{\psi} = \hat{D}(ik_0\boldsymbol{\gamma})$ (eq. (69)) with the basis-independent formulation of the constitutive relation in a linear isotropic medium $\boldsymbol{\gamma} = (\mathbf{I} + \boldsymbol{\chi})\boldsymbol{\psi}$ (eq. (71)) one may write the resulting macroscopic Maxwell's equation in a linear medium as:

$$\nabla \times \boldsymbol{\psi} = ik_0 \hat{D}(\mathbf{I} + \boldsymbol{\chi})\boldsymbol{\psi} \quad (74)$$

which can be written as a homogeneous equation $\mathbf{M}\boldsymbol{\psi} = 0$:

$$\underbrace{\left[ik_0 \hat{D}(\mathbf{I} + \boldsymbol{\chi}) - \begin{pmatrix} \nabla \times & 0 \\ 0 & \nabla \times \end{pmatrix} \right]}_{\mathbf{M}} \boldsymbol{\psi} = 0 \quad (75)$$

This equation can be written, following eq. (28), in the different bases:

$$\begin{aligned} & \left[(k_0\chi_3 - \nabla \times) \begin{pmatrix} 1 & 0 \\ 0 & 1 \end{pmatrix} - ik_0\chi_2 \begin{pmatrix} 1 & 0 \\ 0 & -1 \end{pmatrix} - ik_0\chi_1 \begin{pmatrix} 0 & 1 \\ 1 & 0 \end{pmatrix} - k_0(1 + \chi_0) \begin{pmatrix} 0 & -i \\ i & 0 \end{pmatrix} \right] \begin{pmatrix} \mathbf{F}_e \\ \mathbf{F}_m \end{pmatrix} = \mathbf{0}, \\ & \left[(k_0\chi_3 - \nabla \times) \begin{pmatrix} 1 & 0 \\ 0 & 1 \end{pmatrix} - ik_0\chi_2 \begin{pmatrix} 0 & 1 \\ 1 & 0 \end{pmatrix} - ik_0\chi_1 \begin{pmatrix} 1 & 0 \\ 0 & -1 \end{pmatrix} + k_0(1 + \chi_0) \begin{pmatrix} 0 & -i \\ i & 0 \end{pmatrix} \right] \begin{pmatrix} \mathbf{F}_p \\ \mathbf{F}_a \end{pmatrix} = \mathbf{0}, \\ & \left[(k_0\chi_3 - \nabla \times) \begin{pmatrix} 1 & 0 \\ 0 & 1 \end{pmatrix} - ik_0\chi_2 \begin{pmatrix} 0 & 1 \\ 1 & 0 \end{pmatrix} + ik_0\chi_1 \begin{pmatrix} 0 & -i \\ i & 0 \end{pmatrix} + k_0(1 + \chi_0) \begin{pmatrix} 1 & 0 \\ 0 & -1 \end{pmatrix} \right] \begin{pmatrix} \mathbf{F}_R \\ \mathbf{F}_L \end{pmatrix} = \mathbf{0}. \end{aligned} \quad (76)$$

This reveals under which material parameters will Maxwell's equations be diagonalised for each basis EM, RL or PA—by taking the off diagonal terms to zero in each of the three cases. The conditions are the following.

For EM uncoupled equations,

$$\left\{ \begin{array}{l} 1 + \chi_0 = 0 \\ \chi_1 = 0 \end{array} \right\} \Leftrightarrow \left\{ \begin{array}{l} \varepsilon_r + \mu_r = 0 \\ \varepsilon_r - \mu_r = 0 \end{array} \right\} \Leftrightarrow \left\{ \begin{array}{l} \varepsilon_r(\mathbf{r}) = 0 \\ \mu_r(\mathbf{r}) = 0 \end{array} \right\} \quad \text{with} \quad \begin{array}{l} \chi_c, \chi_t \\ \text{free variables} \end{array} \quad (77)$$

For PA uncoupled equations,

$$\left\{ \begin{array}{l} 1 + \chi_0 = 0 \\ \chi_2 = 0 \end{array} \right\} \Leftrightarrow \left\{ \begin{array}{l} \varepsilon_r + \mu_r = 0 \\ \chi_t = 0 \end{array} \right\} \Leftrightarrow \left\{ \begin{array}{l} \varepsilon_r(\mathbf{r}) = -\mu_r(\mathbf{r}) \\ \chi_t(\mathbf{r}) = 0 \end{array} \right\} \quad \text{with} \quad \begin{array}{l} \chi_c, \mu_r = -\varepsilon_r \\ \text{free variables} \end{array} \quad (78)$$

For RL uncoupled equations,

$$\left\{ \begin{array}{l} \chi_1 = 0 \\ \chi_2 = 0 \end{array} \right\} \Leftrightarrow \left\{ \begin{array}{l} \varepsilon_r - \mu_r = 0 \\ \chi_t = 0 \end{array} \right\} \Leftrightarrow \left\{ \begin{array}{l} \varepsilon_r(\mathbf{r}) = \mu_r(\mathbf{r}) \\ \chi_t(\mathbf{r}) = 0 \end{array} \right\} \quad \text{with} \quad \begin{array}{l} \chi_c, \mu_r = \varepsilon_r \\ \text{free variables} \end{array} \quad (79)$$

The EM uncoupled condition corresponds to ε -and- μ -near-zero (EMNZ) materials [12, 13], well-known to turn Maxwell equations into a quasi-static form and thus uncouple \mathbf{E} from \mathbf{H} . The RL uncoupled condition corresponds to dual materials, $\varepsilon_r(\mathbf{r}) = \mu_r(\mathbf{r})$ (free space being an example), which have been widely discussed as systems that do not perturb the helicity of incoming light, because the right and left-handed components of light are uncoupled [14]. Finally, the PA uncoupled condition $\varepsilon_r(\mathbf{r}) = -\mu_r(\mathbf{r})$ is novel to our knowledge, and it happens for example in a plasma such as a Drude metal with $\mu_r = 1$ and $\varepsilon_r = 1 - \omega_p^2/\omega^2$, at an angular frequency $\omega = \omega_p/\sqrt{2}$ where ω_p is the plasma frequency. It is worth mentioning that in the interface between a material such as vacuum (fulfilling the RL uncoupled condition) and such plasma (fulfilling the PA uncoupled condition) a surface plasmon mode exists theoretically with infinite wavenumber under that exact condition.

Reversing the argument, for any arbitrary linear material defined by $(\chi_0(\mathbf{r}), \chi_1(\mathbf{r}), \chi_2(\mathbf{r}), \chi_3(\mathbf{r}))$ one could in principle diagonalise the macroscopic Maxwell eq. (69), which amounts to finding a basis for the electromagnetic bi-spinor in \mathbb{C}^2 space, in which the equations are uncoupled - but this would need to be done at each point in space \mathbf{r} , due to the position-dependence of the susceptibilities according to the material geometry, in principle limiting the usefulness of this approach. Only in cases where the basis is the same throughout space (as in the cases described above) would this approach be useful. Inside every block of homogeneous material with constant material parameters, an electromagnetic basis in \mathbb{C}^2 space can be found such that its two components are uncoupled. This could represent an interesting approach to solving electromagnetic problems.

RELATION OF QUADRATIC QUANTITIES TO 3D STOKES PARAMETERS

A possible criticism to our main text is the apparently arbitrary choice of the W , \mathbf{S} and \mathbf{T} quadratic quantities to build a framework of quadratic quantities, and not others. We show here that the seemingly arbitrary choice describes a very general situation. A systematic approach to quadratic quantities would be to consider all possible products of all field components with each other. This 'brute force' approach is easily achieved by constructing an outer product in \mathbb{C}^3 space $\mathbf{F}_i^* \otimes \mathbf{F}_i$ between the \mathbf{F}_i vectors from eq. (8) with themselves. This is the approach used by the Stokes-Gell-Mann parameters to characterise 3D polarisation when \mathbf{F}_i is $\sqrt{\varepsilon}\mathbf{E}$ or $\sqrt{\mu}\mathbf{H}$. As we will show, this approach can be decomposed into precisely the quadratic quantities in Table 1 in the main text. First, we note that there are 9 Stokes-Gell-Mann parameters, which happen to be the same amount of degrees of freedom as W_i , \mathbf{S}_i and \mathbf{T}_i , that is, $1 + 3 + 5$ (note $\text{tr } \mathbf{T}_i = -W_i$, which is why it only contributes 5 degrees of freedom). To define 3D Stokes

one usually decomposes $\mathbf{F}_i^* \otimes \mathbf{F}_i$ (where \mathbf{F}_i can be $\sqrt{\varepsilon}\mathbf{E}$ or $\sqrt{\mu}\mathbf{H}$) in terms of Gell-Mann matrices [15, 16]

$$\frac{1}{3} \begin{pmatrix} \Lambda_0 + \Lambda_3 + \frac{1}{\sqrt{3}}\Lambda_8 & \Lambda_1 - i\Lambda_2 & \Lambda_4 - i\Lambda_5 \\ \Lambda_1 + i\Lambda_2 & \Lambda_0 - \Lambda_3 + \frac{1}{\sqrt{3}}\Lambda_8 & \Lambda_6 - i\Lambda_7 \\ \Lambda_4 + i\Lambda_5 & \Lambda_6 + i\Lambda_7 & \Lambda_0 - \frac{2}{\sqrt{3}}\Lambda_8 \end{pmatrix},$$

where the literature is divided on normalisation and also numbering of these parameters. However, our approach is to further decompose this in terms of physical observables. We previously showed that the outer product $\mathbf{F}_i \otimes \mathbf{F}_i^*$ can be written in terms of observables W_i , \mathbf{S}_i and \mathbf{T}_i , see eq. (44). Taking a complex conjugate we get

$$\mathbf{F}_i^* \otimes \mathbf{F}_i = \frac{1}{2}(W_i \mathbf{I} + \mathbf{T}_i + i\omega \star \mathbf{S}_i), \quad (80)$$

which is enough to describe 3D polarisation, and these physically meaningful quadratic quantities contain all the information contained in a brute force approach to quadratics. Also, $\star \mathbf{S}_i$ has a direct geometrical interpretation; it is a plane normal to \mathbf{S}_i (the plane of the polarisation ellipse) with an added sense of rotation determined by the orientation of \mathbf{S}_i (the handedness of the polarisation). To be more explicit, we can write our selection of quadratic quantities, in terms of the corresponding Stokes-Gell-Mann parameters of the $\mathbf{F}_i^* \otimes \mathbf{F}_i$ tensor, as:

$$W_i = \frac{1}{4}\Lambda_0, \quad \mathbf{S}_i = \frac{1}{6\omega} \begin{pmatrix} \Lambda_7 \\ -\Lambda_5 \\ \Lambda_2 \end{pmatrix}, \quad \mathbf{T}_i + W_i \mathbf{I} = \frac{1}{6} \begin{pmatrix} \Lambda_3 + \frac{\Lambda_8}{\sqrt{3}} & \Lambda_1 & \Lambda_4 \\ \Lambda_1 & -\Lambda_3 + \frac{\Lambda_8}{\sqrt{3}} & \Lambda_6 \\ \Lambda_4 & \Lambda_6 & -\frac{2\Lambda_8}{\sqrt{3}} \end{pmatrix} \quad (81)$$

One can confirm by directly using the definitions that:

$$(\mathbf{T}_i + W_i \mathbf{I}) \cdot \mathbf{S}_i = 0, \quad (82)$$

This means that one can find a vector $\hat{\mathbf{e}}_p(\hat{\mathbf{S}}_i)$ and pseudovector $\hat{\mathbf{e}}_s(\hat{\mathbf{S}}_i)$ such that $\hat{\mathbf{e}}_p \cdot \hat{\mathbf{S}}_i = \hat{\mathbf{e}}_s \cdot \hat{\mathbf{S}}_i = \hat{\mathbf{e}}_s \cdot \hat{\mathbf{e}}_p = 0$. These can be used to define a tensor $\hat{\mathbf{e}}_+ = \hat{\mathbf{e}}_p \otimes \hat{\mathbf{e}}_p - \hat{\mathbf{e}}_s \otimes \hat{\mathbf{e}}_s$ and a pseudotensor $\hat{\mathbf{e}}_\times = \hat{\mathbf{e}}_s \otimes \hat{\mathbf{e}}_p + \hat{\mathbf{e}}_p \otimes \hat{\mathbf{e}}_s$ that form a basis of all symmetric tensors perpendicular to $\hat{\mathbf{S}}_i$ (satisfying eq. (82)). This basis allows for a surprisingly simple form in terms of the observables, if $\text{sgn}(\mathbf{p}_i \cdot \mathbf{S}_i) = \pm 1$:

$$\begin{aligned} 4W_i &= \mathcal{S}_0, & 4\omega \mathbf{S}_i &= \pm \mathcal{S}_3 \hat{\mathbf{S}}_i, \\ 4(\mathbf{T}_i + W_i \mathbf{I}) &= -\mathcal{S}_1 \hat{\mathbf{e}}_+ \mp \mathcal{S}_2 \hat{\mathbf{e}}_\times, \end{aligned} \quad (83)$$

where \mathcal{S}_A are the usual 2D Stokes parameters calculated for the vector \mathbf{F}_i in the plane to which $\hat{\mathbf{S}}_i$ is normal to (plane of polarisation ellipse). Notice that we never assumed a paraxial beam; therefore, eq. (83) is true for an arbitrary field with $\mathbf{S}_i \neq \mathbf{0}$. Inverting it we get the four Stokes parameters

$$\begin{aligned} \mathcal{S}_0 &= -4 \text{tr}(\mathbf{T}_i) = 4W_i, & \mathcal{S}_2 &= \mp 2 \text{tr}(\hat{\mathbf{e}}_\times \cdot \mathbf{T}_i), \\ \mathcal{S}_1 &= -2 \text{tr}(\hat{\mathbf{e}}_+ \cdot \mathbf{T}_i), & \mathcal{S}_3 &= \pm 4\omega |\mathbf{S}_i|, \end{aligned} \quad (84)$$

with two additional real angles sufficient to specify the 3D orientation of \mathbf{S}_i and hence the orientation of the plane where the above Stokes parameters are defined. This represents a simple approach to describe the three-dimensional polarisation of the \mathbf{F}_i field based only on the quadratic quantities W_i , \mathbf{S}_i and \mathbf{T}_i . Notice that we only have six degrees of freedom (four Stokes parameters plus two angles for the orientation of vector \mathbf{S}_i), we started with nine, but eq. (82) contains three constraints.

For example, the linear Stokes parameters for the vector $\mathbf{F}_i = \mathbf{F}_e = (1/2)\sqrt{\varepsilon}\mathbf{E}$ and spin $\mathbf{S}_i = \mathbf{S}_e$, assuming that the spin is not aligned with the z -axis (in which case they would coincide with the usual definition) and assuming a choice of basis vectors $\hat{\mathbf{e}}_s$ and $\hat{\mathbf{e}}_p$ that matches with the polar and azimuthal unit vectors in spherical coordinates (also called s-polarised and p-polarised) with respect to a spin vector \mathbf{S}_i taken as radial (and hence satisfying the required orthogonality $\hat{\mathbf{e}}_p \cdot \hat{\mathbf{S}}_i = \hat{\mathbf{e}}_s \cdot \hat{\mathbf{S}}_i = \hat{\mathbf{e}}_s \cdot \hat{\mathbf{e}}_p = 0$) will be uniquely given by components of observables W_e , \mathbf{S}_e and \mathbf{T}_e :

$$\begin{aligned} \mathcal{S}_1 &= 4(W_{ex} + W_{ey}) - 4W_{ez} \frac{4\omega^2 S_{ez}^2}{4(W_{ex} + W_{ey})W_{ez} - T_{exz}^2 - T_{eyz}^2 + \omega^2(S_{ey}^2 + S_{ex}^2)} \\ \mathcal{S}_2 &= \pm \frac{4}{|\mathbf{S}_e|} \left\{ S_{ex} T_{eyz} - S_{ey} T_{exz} + \frac{S_{ez}}{S_{ex}^2 + S_{ey}^2} [2S_{ex} S_{ey} (W_{ex} - W_{ey}) - T_{exy} (S_{ex}^2 - S_{ey}^2)] \right\}. \end{aligned} \quad (85)$$

ACKNOWLEDGEMENTS

SG and FJRF acknowledge support from EIC-Pathfinder-CHIRALFORCE (101046961) which is funded by Innovate UK Horizon Europe Guarantee (UKRI project 10045438). AJV is supported by EPSRC Grant EP/R513064/1.

* sebastian.1.golat@kcl.ac.uk

† francisco.rodriguez_fortuno@kcl.ac.uk

- [1] P. Lounesto, Clifford algebras and spinors, in *Clifford Algebras and Their Applications in Mathematical Physics* (Springer, 2001) pp. 37–39.
- [2] M. Nieto-Vesperinas and X. Xu, The complex maxwell stress tensor theorem: The imaginary stress tensor and the reactive strength of orbital momentum. a novel scenery underlying electromagnetic optical forces, *Light: Science & Applications* **11**, 297 (2022).
- [3] J. D. Jackson, *Classical Electrodynamics* (John Wiley and Sons Ltd, 1998).
- [4] J. E. S. Bergman and T. D. Carozzi, Canonical electromagnetic observables for systematic characterization of electric and magnetic wave field data on board spacecraft (2009), [arXiv:0804.2092](https://arxiv.org/abs/0804.2092) [physics.geo-ph].
- [5] K. Y. Bliokh, Y. S. Kivshar, and F. Nori, Magnetolectric effects in local light-matter interactions, *Phys. Rev. Lett.* **113**, 033601 (2014).
- [6] M. Nieto-Vesperinas and X. Xu, Reactive helicity and reactive power in nanoscale optics: Evanescent waves. kerker conditions. optical theorems and reactive dichroism, *Physical Review Research* **3**, 043080 (2021).
- [7] E. Kamenetskii, M. Berezin, and R. Shavit, Microwave magnetolectric fields: helicities and reactive power flows, *Applied Physics B* **121**, 31–47 (2015).
- [8] A. J. Vernon, S. Golat, C. Rigouzzo, E. A. Lim, and F. J. Rodríguez-Fortuño, A decomposition of light’s spin angular momentum density (2023), [arXiv:2310.03804](https://arxiv.org/abs/2310.03804) [physics.optics].
- [9] M. F. Picardi, A. V. Zayats, and F. J. Rodríguez-Fortuño, Janus and Huygens dipoles: Near-field directionality beyond spin-momentum locking, *Physical Review Letters* **120**, 117402 (2018).
- [10] A. J. Vernon, A. Kille, F. J. Rodríguez-Fortuño, and A. Afanasev, Non-diffracting polarization features around far-field zeros of electromagnetic radiation, *Optica* **11**, 120 (2024).
- [11] E. A. Muljarov and T. Weiss, Resonant-state expansion for open optical systems: generalization to magnetic, chiral, and bi-anisotropic materials, *Optics letters* **43**, 1978–1981 (2018).
- [12] R. W. Ziolkowski, Propagation in and scattering from a matched metamaterial having a zero index of refraction, *Physical Review E* **70**, 046608 (2004).
- [13] A. M. Mahmoud and N. Engheta, Wave-matter interactions in epsilon-and-mu-near-zero structures, *Nature communications* **5**, 5638 (2014).
- [14] X. Zambrana-Puyalto, I. Fernandez-Corbaton, M. Juan, X. Vidal, and G. Molina-Terriza, Duality symmetry and kerker conditions, *Optics letters* **38**, 1857–1859 (2013).
- [15] T. Carozzi, R. Karlsson, and J. Bergman, Parameters characterizing electromagnetic wave polarization, *Physical Review E* **61**, 2024 (2000).
- [16] T. Setälä, A. Shevchenko, M. Kaivola, and A. T. Friberg, Degree of polarization for optical near fields, *Physical Review E* **66**, 016615 (2002).